Copper content in ascitic fluid is associated with angiogenesis and progression in ovarian cancer
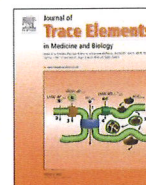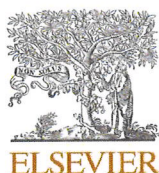
メタデータ	言語: English
	出版者:
	公開日: 2023-08-02
	キーワード (Ja):
	キーワード (En):
	作成者: 大沼, 利通
	メールアドレス:
	所属:
URL	http://hdl.handle.net/10098/0002000004

Copper content in ascitic fluid is associated with angiogenesis and progression in ovarian cancer

Toshimichi Onuma [a], Tetsuya Mizutani [b], Yuko Fujita [a], Shizuka Yamada [a], Yoshio Yoshida [a,*]

[a] *Department of Obstetrics and Gynecology, Faculty of Medical Sciences, University of Fukui, Fukui, 910-1193, Japan*
[b] *Department of Nursing, Faculty of Nursing and Welfare Sciences, Fukui Prefectural University, Fukui, 910-1195, Japan*

ARTICLE INFO

ABSTRACT

Background: Ascites is associated with the poor prognosis of malignant tumors. The biological importance of the changes in the content of trace elements in the ascitic fluid is unknown. Herein, we analyzed trace elements in the ascitic fluid of patients with ovarian tumors and used cultured cells to determine the copper (Cu)-induced changes in gene expression in ovarian cancer.

Methods: Inductively coupled plasma mass spectrometry (ICP-MS) was used to compare ascitic fluid trace element levels in patients with benign ovarian tumors ($n = 22$) and borderline/malignant tumors ($n = 5$) for primary screening. Cu levels were validated using atomic absorption spectrometry (AAS) in 88 benign, 11 borderline, and 25 malignant ovarian tumor patients. To confirm Cu-induced gene expression changes, microarray analysis was performed for Cu-treated OVCAR3, A2780, and Met5A cells. The vascular endothelial growth factor (VEGF) concentration in the cell supernatant or ascitic fluid (ovarian cancer samples) was measured using ELISA.

Results: ICP-MS showed that Co, Ni, Cu, Zn, As, Se, and Mo levels significantly increased in patients with malignant/borderline ovarian tumors compared to those in patients with benign ovarian tumors. AAS showed that malignant ovarian tumors were independently associated with elevated levels of Cu in ascites adjusted for age, body mass index, alcohol, smoking, and supplement use ($p < 0.001$). Microarray analysis of both Cu-treated ovarian cancer cell lines OVCAR3 and A2780 and the mesothelial cell line Met-5A revealed the upregulation of the angiogenesis biological process. Real-time polymerase chain reaction and ELISA demonstrated that an increased Cu content significantly enhanced *VEGF* mRNA expression and protein secretion in OVCAR3, A2780, and Met-5A cells. VEGF levels and clinical stages of the tumors correlated with the ascitic fluid Cu content in patients with malignant ovarian tumors (correlation coefficient 0.445, 95 % confidence interval [CI]: 0.069–0.710, $p = 0.023$ and correlation coefficient 0.406, 95 % CI: 0.022–0.686, $p = 0.040$, respectively).

Conclusion: Cu levels significantly increased in patients with malignant ovarian cancer. Cu induced angiogenic effects in ovarian cancer and mesothelial cells, which affected ascites fluid production. This study clarifies the link between elevated Cu in ascites and malignant ovarian tumor progression. Strategies to decrease Cu levels in the ascitic fluid may help downregulate VEGF expression, thereby improving the prognosis of ovarian malignancies.

1. Introduction

The presence of ascites is associated with poor prognosis of several malignancies. More than one-third of patients with ovarian cancer develop ascites during cancer development or treatment [1]. The median progression-free survival and 5-year survival rate of advanced ovarian cancer (stage III or IV) remain at 16–22 months and 27 %, respectively, indicating poor prognosis [2]. Therefore, new therapeutic strategies for improving the prognosis of ovarian cancer are urgently needed.

Trace elements play important roles in homeostasis and their levels are tightly regulated. A deficiency of trace elements exacerbates or leads to the development of various diseases. Trace elements also become harmful when their concentrations exceed physiological levels [3]. Although the presence of harmful metals such as Al, As and Cd are associated with pathological conditions [4], there are also reports indicating that harmful metals are associated with cancer [5–7].

Although ascites is closely associated with the prognosis of malignant diseases, only one report has described the presence of trace elements in ascites of patients with malignancies [8]. Some reports have comprehensively examined the effects of changes in trace elements on differential gene expression in malignant tumors, including ovarian cancer, with most studies having used serum and nail samples [7,9–11]. However, no studies have reported the presence of trace elements in ascites from ovarian cancer using multi-trace element determination.

Copper (Cu) is an essential trace element and a coenzyme for cuproenzymes involved in embryogenesis, growth, homeostasis, and angiogenesis [12,13]. Cu is also associated with the development of malignancies, including ovarian tumors. Increased serum Cu levels are observed in various types of malignant tumors and are associated with the advanced stage of malignant tumors [14]. Cu-binding proteins have also been associated with malignant tumors. Lee et al. showed that Copper Transporter (CTR) 1 and CTR2 exhibit decreased expression in ovarian cancer cells and that low CTR1 is associated with chemotherapy resistance and poor prognosis of ovarian cancer patients [15]. These findings highlight the relevance of copper dynamics in cancer progression.

Herein, we hypothesized that alterations in the ascitic fluid Cu levels can influence the progression of ovarian cancer. Our study clarifies, for the first time, the link between elevated Cu in ascites and malignant ovarian tumor progression using cultured cells and clinical specimens.

2. Materials and methods

2.1. Patient enrollment for trace element determination

Patients who underwent surgery for ovarian tumors at the Fukui University Hospital in 2014–2019 were enrolled in this study. All patients stopped taking supplements and over-the-counter drugs more than two weeks prior to surgery. The exclusion criteria were as follows: presence of infectious bacterial peritonitis, renal failure, and liver cirrhosis; ongoing corticosteroid treatment and usage of immunosuppressive agents; ongoing chemotherapy before sample collection; and presence of metastatic ovarian cancer. Enrolled patients provided written informed consent to participate in the study. We obtained ascitic fluid from the Douglas pouch using a suction tube immediately after peritoneal incision during surgery. We transferred the ascitic fluid into 15-mL polyethylene tubes, which were stored at -80 °C until determination. This study was approved by the ethics review board of Fukui University Hospital (approval no. 20160021).

2.2. Multielement determination of Ascitic Fluid using inductively coupled plasma mass spectrometry (ICP-MS)

For primary trace element screening in ascites, ascitic fluid from 22 patients with benign tumors and four patients with malignant/borderline tumors, who underwent surgery between 2014 and 2016 (Supplementary Table S1), was analyzed as described previously [16]. The histological features of ovarian tumors are shown in Supplementary table S1. Briefly, ascites samples were placed in 15-mL polyethylene tubes containing 2 mL nitric acid (61 %; Kanto Chemical, Tokyo, Japan). The tubes were incubated at 80 °C for 3 h followed by cooling for 1 h. Next, 1.0 mL hydrogen peroxide (30 %; Kanto Chemical) was added to each tube, and the tubes were incubated at 80 °C for 3 h. After dilution of the digested materials with Milli-Q water, Al, Co, Ni, Cu, Zn, As, Se, Mo, Cd, Sb, Ba, and Pb levels were determined by ICP-MS (Agilent 7500cx,

Agilent Technologies, Santa Clara, CA, USA). The levels of all elements, except Se was measured in He mode; Se was measured in H_2 mode.

2.3. Detection of Cu in ascitic fluid of ovarian tumor

Ascites Cu in patients who underwent surgery between 2016 and 2019 was measured using atomic absorption spectrometry (AAS, ZA3000, Hitachi High-Tech Science, Tokyo, Japan). The histological features of 88 benign, 11 borderline, and 26 malignant ovarian tumors are shown in Supplementary Tables S2–S4. The samples were transferred to acid-washed test tubes, and the Cu concentration was determined by measuring the absorbance at 324.8 nm.

2.4. Materials and cell culture

We purchased the Met-5A mesothelial cell line and the ovarian cancer cell lines OVCAR3 (serous carcinoma) and A2780 (endometrioid carcinoma) from the American Type Culture Collection (Manassas, VA, USA). The cells were cultured in RPMI-1640 (Wako, Osaka, Japan) supplemented with 10 % fetal bovine serum (Biowest, Nuaillé, France) and 1.0 % penicillin/streptomycin (Gibco, Grand Island, NY, USA) at 37 °C and 5% CO_2. $CuSO_4$ was purchased from Sigma-Aldrich, (St. Louis, MO, USA), and a 100 mM $CuSO_4$ stock solution was prepared in distilled water.

2.5. Microarray analysis

Met-5A, OVCAR3, and A2780 cells (10^6 cells) were grown for 48 h. Next, the culture medium was removed, and the cells were treated with fresh medium containing 0 or 200 µM Cu for 4 h (previous studies have described serum copper levels of up to 200 µM in cancer patients [14, 17]). Total RNA was extracted from the cells using a RNeasy Kit (Qiagen, Hilden, Germany) according to the manufacturer's instructions. We confirmed the RNA quality using an Agilent 2100 bioanalyzer. The RNA integrity for all samples ranged from 9.8–10.0, which was adequate for microarray. Microarray was performed using the Clariom S Assay (Applied Biosystems, Foster City, CA, USA) according to the manufacturer's instructions. The data were analyzed using the Subio Platform (Subio, Inc., Tokyo, Japan). Each signal was log-transformed followed by background correction and normalization. We defined differentially expressed genes (DEGs) based on the following criteria: (1) expression >1.5-fold between 0 and 200 µM Cu-treated cells, and (2) $p < 0.1$ (two-sided t-test) between the 0 and 200 µM Cu-treated cells. We performed gene ontology enrichment analysis using the PANTHER functional annotation web tool (http://pantherdb.org/) to identify the associated pathway and biological process. Lists of DEG symbols were entered into the PANTHER database to classify genes into functional groups, thereby providing information on the pathways. The PANTHER statistical over- and under- representation tests were conducted using DEG symbols to determine whether the identified biological processes were statistically over- or under-expressed [18].

2.6. Gene expression analysis

Met-5A, OVCAR3, and A2780 cells (10^6 cells) were grown for 48 h followed by treatment with medium containing 0, 20, and 200 µM Cu for 4 and 24 h. Total RNA was extracted from all cells using a RNeasy Kit according to the manufacturer's instructions. The cDNA was synthesized using the SuperScript IV VILO Master Mix kit (Invitrogen, Carlsbad, CA, USA) and amplified using the Power SYBR Green Master Mix kit (Applied Biosystems) with primers targeting gene sequences for *36B4* and vascular endothelial growth factor (*VEGF*) according to the manufacturer's instructions. Gene expression was quantified and analyzed using real-time polymerase chain reaction (real-time PCR) on the Step One Plus system (Applied Biosystems) following the manufacturer's instructions. The following gene-specific primers were used: 36B4

forward, 5′-GCTGCAGCCCCAGCTAAGGT-3′; 36B4 reverse, 5′-TAAGTTGGTTGCTTTTTGGT-3′; VEGF forward, 5′-AGGGCAGAATCATCACGAAGT-3′; and VEGF reverse, 5′-AGGGTCTCGATTGGATGGCA-3′ [19]. *VEGF* expression was normalized to that of *36B4*, and the mRNA levels were presented as the fold-change. Untreated cells were used as a control. Experiments and assays were performed 3–5 times.

2.7. VEGF protein levels

Met-5A, OVCAR3, and A2780 cells (10^6 cells) were grown for 48 h followed by incubation with 5.0 mL of fresh medium containing 0, 20, and 200 µM Cu for 4 and 24 h. The culture medium was collected. VEGF protein was measured using the Quantikine Human VEGF Immunoassay kit (R&D Systems, Minneapolis, MN, USA) as per the manufacturer's instructions. Total protein was quantified using the Bradford protein assay kit (Bio-Rad, Hercules, CA, USA) according to the manufacturer's instructions. VEGF was expressed as a percentage of the total protein and fold-change based on Cu at 0 µM [20]. All measurements were performed in triplicate. Ascitic fluid samples from patients with ovarian cancer were collected and stored at -80 °C until determination, and VEGF levels were measured using the same immunoassay kit. The histological features of 26 malignant tumors are shown in Supplementary Table S4.

2.8. Statistical analysis

Student's *t*-test, Mann–Whitney *U* test, one-way analysis of variance adjusted using Dunnett's method and the Kruskal–Wallis rank-sum test adjusted using the Steel method were used to compare the continuous variables. The Fisher's exact test adjusted with the Bonferroni method was used to compare the proportions for categorical variables. Multivariable linear regression analysis models were created to analyze the association of the ascitic fluid Cu concentration measured using AAS with benign, borderline, or malignant ovarian tumors. Spearman's test was performed to analyze the correlation between VEGF expression and clinical stage or ascitic fluid Cu concentration in malignant ovarian tumors. Statistical analyses, except for microarray, were performed with EZR (Saitama Medical Center, Jichi Medical University, Saitama, Japan), a graphical user interface for R (The R Foundation for Statistical Computing, Vienna, Austria) [21]. A $p < 0.05$ was considered as statistically significant, except for microarray analysis.

3. Results

3.1. Increased concentration of various trace elements in ascitic fluid of malignant tumors

Table 1 and Supplementary Fig. S1−12 presents the results of multielement determination of ascitic fluid samples obtained from patients with benign and borderline/malignant ovarian tumors obtained by ICP-MS. There were no significant differences between patients with benign and borderline/malignant tumors in terms of age, menopause rate, body mass index (BMI), smoking, alcohol, or supplement use. According to the ICP-MS results, Co, Ni, Cu, Zn, As, Se, and Mo levels were significantly increased in borderline/malignant ovarian tumors compared to benign ovarian tumors ($p < 0.05$). These results suggest that the various trace elements in ascites were associated with malignant tumor progression.

3.2. Malignant ovarian tumors associated with increased Cu concentration in Ascites

The levels of many trace elements were increased in the ascitic fluid of patients with malignant tumors in the primary trace element screening. Increased serum Cu levels are associated with malignant

Table 1

Multi-trace element analysis of ascitic fluid samples obtained from different types of ovarian tumors by ICP-MS.

	Benign	Borderline/Malignant	*p* value
n	22	5	
Age median (range) years[a]	44.5 (25–79)	48 (39–68)	0.453
Menopause % (*n*) [b]	22.7 (5)	40 (2)	0.580
BMI median (range) kg/m[a,b]	22.4 (17–36)	23.1 (18.1–32)	0.574
Smoke % (*n*)[b]	36.4 (8)	0 (0)	0.280
Alcohol % (*n*)[b]	50 (11)	20 (1)	0.342
Supplement % (*n*)[b]	36.4 (8)	2 (40)	1.000
Element median (range) ppb[a]			
Al	32.67 (12.49–176.29)	38.80 (24.39–98.49)	0.976
Co	1.27 (0.36–5.04)	6.85 (6.40–17.82)	0.013
Ni	42.74 (37.61–85.02)	67.61 (44.96–73.79)	0.023
Cu	565.94 (369.11–776.48)	811.21 (443.96–952.73)	0.023
Zn	312.10 (163.11–5996.14)	3671.77 (259.30–5501.20)	0.047
As	2.71 (1.20–8.86)	3.9 (2.06–19.62)	0.257
Se	75.09 (41.54–108.52)	85.25 (73.93–113.20)	0.040
Mo	1.90 (1.16–4.19)	2.95 (2.59–15.15)	0.010
Cd	0.50 (0.11–22.29)	2.33 (0.33–18.58)	0.113
Sb	0.26 (0.14–1.89)	0.35 (0.54–9.08)	0.064
Ba	1.72 (0.54–7.93)	3.31 (1.26–34.18)	0.129
Pb	0.65 (0.29–4.01)	1.26 (0.62–10.33)	0.086

[a] Mann–Whitney *U* test was used for statistical analysis.
[b] Fisher's exact test was used for statistical analysis. ICP-MS, inductively coupled plasma mass spectrometry; BMI, body mass index.

ovarian tumors [9]. For our primary screen, we divided the ovarian tumors into benign and malignant tumors, with the borderline ovarian tumors included in the malignant group because of their low malignant potential [35]. In our deeper analysis of the relationship between ovarian tumors and copper in ascites, using AAS measurements, we divided the ovarian tumors into benign, borderline, and malignant groups to ensure a more comprehensive analysis. There was no significant difference in the ascitic fluid Cu concentration between patients with benign and borderline ovarian tumors ($p = 0.50$). However, patients with malignant ovarian tumors exhibited increased ascitic fluid Cu concentration compared to those with benign ovarian tumors ($p < 0.001$; Table 2). We performed multivariable linear regression analysis of the Cu concentration in ascitic fluid from patients with benign, borderline, and malignant ovarian tumors using AAS (Table 3). Patients

Table 2

Patient characteristics and ascite Cu levels (measured using atomic absorption spectrometry) during validation analysis.

Disease groups	Benign	Borderline	Malignant	*p* value
n	88	11	26	
Age, years, mean (SD)[a]	40.9 (15.1)	54.9 (18.6)	52.9 (12.1)	<0.001
Menopause % (*n*)[b]	18.2 (16)	54.5(6)	57.7 (15)	<0.001
BMI, kg/m², mean (SD)[a]	22.4	22.9	23.8 (4.6)	0.259
Smoking[b]				0.967
Never % (*n*)	76.1 (67)	81.8 (9)	84.6 (22)	
Current % (*n*)	11.4 (10)	9.1 (1)	7.7 (2)	
Past % (*n*)	12.5 (11)	9.1 (1)	7.7 (2)	
Alcohol % (*n*)[b]	43. 2(38)	54.5 (6)	26.9 (7)	0.201
Supplement % (*n*)[b]	28.4 (25)	18.2 (2)	15.4 (4)	0.391
Ascites Cu, ppb, median[c]	596.6	720.0	878.1	<0.001
Range	12–141	28–186	24–139	

[a] One-way ANOVA adjusted using the Holm method was used for statistical analysis.
[b] Fisher's exact test adjusted using the Holm method was used for statistical analysis.
[c] Kruskal–Wallis rank-sum test adjusted using the Steel method was used for statistical analysis. BMI, body mass index; SD, standard deviation.

Table 3
Multivariate linear regression analysis of Cu concentration in ascites from patients with ovarian cancer.

	Unadjusted	p value	Model 1	p value	Model 2	p value
Borderline Regression coefficient (95 % CI)	1.126 (0.893–1.421)	0.313	1.136 (0.897–1.438)	0.288	1.158 (0.915–1.466)	0.220
Malignant Regression coefficient (95 % CI)	1.447 (1.231–1.702)	<0.001	1.436 (1.207–1.708)	<0.001	1.452 (1.225–1.721)	<0.001

Cu concentrations were log-transformed to ensure normality. The regression coefficient was calculated for benign ovarian tumors. Model 1 was adjusted for age, BMI, alcohol, smoking, and supplement use. Model 2 was adjusted for menopause, BMI, alcohol, smoking, and supplement use. CI, confidence interval.

with malignant ovarian tumors showed a significant difference in the adjusted regression coefficient of ascites Cu concentration compared to those with benign ovarian tumors (model 1: $p < 0.001$ and model 2: $p < 0.001$). These results indicate that ovarian cancer was independently associated with elevated Cu levels in ascitic fluid.

3.3. Cu-induced DEGs are involved in promoting angiogenesis in ovarian Cancer and mesothelial cells

Microarray was performed to determine the Cu-induced DEGs. As ovarian cancer and mesothelial cells are associated with ascites production [2], OVCAR3 and A2780 cells were used as ovarian cancer cells and Met-5A cells were used as mesothelial cells. The list of upregulated DEGs (A2780 634, OVCAR3 1110 and Met5A 580 genes) were entered into the PANTHER pathways analysis website and Met5A 70 pathways, OVCAR3 95 pathways, and A2780 75 pathways were identified (Fig. 1A-C and Supplementary Tables S5-S7). Angiogenesis (P00005), p53 pathway (P00059), and oxidative stress response (P00046) were included in all cell lines. The PANTHER statistical over- and under-representation test was conducted on the upregulated DEGs. Tables 4–6 list the top 30 enriched GO-Slim Biological Processes with a false discovery rate adjusted p value of < 0.05. The DEGs for all biological processes are listed in Supplementary Tables S8-S10. The responses to cadmium ion (GO:0046686), cellular zinc ion homeostasis (GO:0006882), and cellular transition metal ion homeostasis (GO:0046916) were included for all cell lines. Additionally, the angiogenesis biological process was also included in all cell lines (Met-5A; positive regulation of angiogenesis GO:0045766, OVCAR3, and A2780; and regulation of angiogenesis GO:0045765).

3.4. Cu-induced VEGF expression in ovarian Cancer and mesothelial cells

We analyzed VEGF expression, as the pathway and biological process for angiogenesis were activated and included VEGF in all cell lines (Supplementary Table S8−10). VEGF mRNA levels were increased in all cell lines in response to 4-h and 24-h incubations with 200 μM Cu ($p < 0.05$, Fig. 2A and B) compared to the VEGF mRNA levels without Cu.

This agreed with the microarray data and indicated a correlation between Cu and upregulation of VEGF expression. VEGF protein levels in the supernatant of OVCAR3 and Met-5A cells treated with Cu (200 μM, 4 h) increased significantly compared with those in cells treated with 0 μM of Cu (OVCAR3 and Met-5A, p < 0.05, Fig. 2C). Compared to treatment with 0 μM of Cu, treatment with 200 μM of Cu for 24 h increased VEGF protein levels in all cell lines ($p < 0.05$, Fig. 2D), indicating the role of Cu in enhancing the expression and extracellular secretion of VEGF.

3.5. Cu concentration in ascitic fluid correlated with ascitic fluid VEGF level in malignant ovarian tumors

Next, we examined the correlation between the Cu concentration and tumor progression or VEGF levels in the ascitic fluid of patients with malignant ovarian tumor. The histological type and clinical stage for all malignant ovarian tumors are shown in Table S4. In total, 26.9 % (7/25) and 38.5 % (10/26) patients had serous cancer and stage III or IV advanced cancer, respectively. The median VEGF level in the ascitic fluid was 225.5 pg/mL (range 15.6–29,500 pg/mL). Fig. 3 shows the correlation between the ascitic VEGF levels, ascitic fluid Cu content, and clinical stage of the tumor. The ascitic fluid Cu content correlated with clinical stage ($p = 0.023$; Fig. 3A). However, the clinical stage did not correlate with VEGF protein levels in the ascitic fluid ($p = 0.168$; Fig. 3B). The Cu concentration in the ascitic fluid positively correlated with the VEGF protein concentration in the ascitic fluid ($p = 0.040$; Fig. 3C). Therefore, the Cu content in the ascitic fluid correlated with ovarian cancer progression and VEGF protein levels, similar to that in the supernatant of Cu-treated cells.

4. Discussion

In this study, we performed ICP-MS to analyze samples from patients with malignant, borderline, and benign ovarian tumors to identify trace elements in the ascitic fluid associated with malignant ovarian tumors in a primary screening. Co, Ni, Cu, Zn, As, Se, and Mo levels were higher in malignant and borderline ovarian tumors than in benign tumors. The Cu level in ascitic fluid was independently associated with malignant
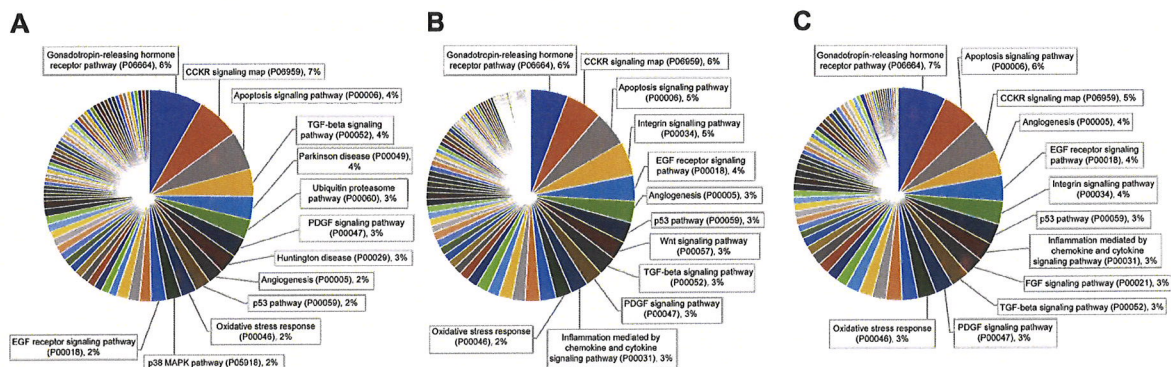

Fig. 1. PANTHER pathway categories identified in A2780, OVCAR3, and Met-5A cells.
Pie charts showing the Panther pathway categories derived from DEGs in all cell lines (A. A2780, B. OVCAR3, and C. Met-5A). The full index lists of these Panther pathway categories are listed in Supplementary Table S5-S7.

Table 4
Thirty most-enriched GO-Slim Biological Processes in A2780.

No.	PANTHER GO-Slim Biological Process	Genes *	over +/under-	p value[†]
1	response to cadmium ion (GO:0046686)	10	+	6.37E-09
2	cellular zinc ion homeostasis (GO:0006882)	11	+	1.48E-07
3	response to toxic substance (GO:0009636)	10	+	8.87E-07
4	chaperone-mediated protein folding (GO:0061077)	9	+	7.06E-06
5	protein demethylation (GO:0006482)	4	+	1.26E-02
6	'de novo' protein folding (GO:0006458)	7	+	2.22E-04
7	cellular transition metal ion homeostasis (GO:0046916)	13	+	3.83E-08
8	transition metal ion homeostasis (GO:0055076)	14	+	3.61E-08
9	circadian regulation of gene expression (GO:0032922)	4	+	2.91E-02
10	negative regulation of MAP kinase activity (GO:0043407)	4	+	3.26E-02
11	response to metal ion (GO:0010038)	10	+	8.10E-05
12	response to unfolded protein (GO:0006986)	8	+	6.98E-04
13	cellular response to unfolded protein (GO:0034620)	8	+	6.90E-04
14	circadian rhythm (GO:0007623)	5	+	1.53E-02
15	rhythmic process (GO:0048511)	5	+	1.96E-02
16	regulation of angiogenesis (GO:0045765)	4	+	4.93E-02
17	negative regulation of MAPK cascade (GO:0043409)	4	+	4.91E-02
18	regulation of vasculature development (GO:1901342)	4	+	4.88E-02
19	response to inorganic substance (GO:0010035)	11	+	8.03E-05
20	cellular response to topologically incorrect protein (GO:0035967)	9	+	6.25E-04
21	response to topologically incorrect protein (GO:0035966)	9	+	6.17E-04
22	regulation of MAP kinase activity (GO:0043405)	9	+	1.27E-03
23	phospholipid dephosphorylation (GO:0046839)	5	+	4.46E-02
24	negative regulation of protein kinase activity (GO:0006469)	6	+	2.20E-02
25	negative regulation of protein phosphorylation (GO:0001933)	7	+	1.24E-02
26	negative regulation of kinase activity (GO:0033673)	6	+	2.43E-02
27	negative regulation of transferase activity (GO:0051348)	6	+	2.65E-02
28	negative regulation of phosphorylation (GO:0042326)	7	+	1.49E-02
29	regulation of protein serine/threonine kinase activity (GO:0071900)	11	+	1.57E-03
30	cellular response to external stimulus (GO:0071496)	6	+	4.17E-02

GO, gene ontology.
[†] False discovery rate adjusted p-value.
[*] Number of genes included in the biological process.

Table 5
Thirty most-enriched GO-Slim Biological Processes in OVCAR3.

No.	PANTHER GO-Slim Biological Process	Genes *	over +/under -	fold Enrichment	p value[†]
1	response to cadmium ion (GO:0046686)	9	+	14.36	1.28E-05
2	regulation of epithelial cell differentiation (GO:0030856)	3	+	12.44	3.89E-02
3	negative regulation of MAP kinase activity (GO:0043407)	9	+	10.37	5.73E-05
4	epidermis development (GO:0008544)	5	+	10.37	5.13E-03
5	epidermal cell differentiation (GO:0009913)	4	+	10.37	1.65E-02
6	peptidyl-tyrosine dephosphorylation (GO:0035335)	6	+	8.89	2.92E-03
7	negative regulation of MAPK cascade (GO:0043409)	9	+	8.89	1.24E-04
8	positive regulation of apoptotic signaling pathway (GO:2001235)	4	+	8.3	2.76E-02
9	cellular zinc ion homeostasis (GO:0006882)	11	+	8.15	3.08E-05
10	signal transduction by p53 class mediator (GO:0072331)	4	+	7.54	3.50E-02
11	response to toxic substance (GO:0009636)	9	+	7.18	3.74E-04
12	'de novo' protein folding (GO:0006458)	7	+	6.91	3.02E-03
13	protein demethylation (GO:0006482)	4	+	6.91	4.33E-02
14	extrinsic apoptotic signaling pathway via death domain receptors (GO:0008625)	5	+	6.91	1.77E-02
15	cellular transition metal ion homeostasis (GO:0046916)	13	+	6.74	2.18E-05
16	chaperone-mediated protein folding (GO:0061077)	8	+	6.64	1.43E-03
17	regulation of MAP kinase activity (GO:0043405)	17	+	6.3	1.56E-06
18	icosanoid metabolic process (GO:0006690)	5	+	6.1	2.61E-02
19	negative regulation of kinase activity (GO:0033673)	12	+	5.93	1.18E-04
20	transition metal ion homeostasis (GO:0055076)	14	+	5.93	2.72E-05
21	negative regulation of transferase activity (GO:0051348)	12	+	5.79	1.35E-04
22	positive regulation of response to DNA damage stimulus (GO:2001022)	5	+	5.76	3.02E-02
23	negative regulation of phosphorylation (GO:0042326)	14	+	5.69	3.67E-05
24	negative regulation of protein kinase activity (GO:0006469)	11	+	5.56	3.55E-04
25	negative regulation of protein phosphorylation (GO:0001933)	13	+	5.5	9.64E-05
26	regulation of apoptotic signaling pathway (GO:2001233)	8	+	5.03	5.70E-03
27		5	+	4.94	

ovarian tumor. To investigate the significance of the increased Cu levels in the ascitic fluid, we used ovarian cancer cell lines, OVCAR3 and A2780, and mesothelial cells, Met-5A cell line. Microarray analysis using PANTHER showed that upregulated DEGs were associated with the pathways and the biological processes involved in angiogenesis. Cu upregulated *VEGF* expression and its extracellular secretion in OVCAR3, A2780, and Met-5A cells. Further, the clinical cancer stage and VEGF concentration were correlated with the ascitic fluid Cu content in

Table 5 (*continued*)

No.	PANTHER GO-Slim Biological Process	Genes *	over +/under -	fold Enrichment	p value[†]
	regulation of angiogenesis (GO:0045765)				4.85E-02
28	epidermal growth factor receptor signaling pathway (GO:0007173)	5	+	4.94	4.84E-02
29	regulation of vasculature development (GO:1901342)	5	+	4.94	4.82E-02
30	unsaturated fatty acid metabolic process (GO:0033559)	5	+	4.94	4.80E-02

GO, gene ontology.

[†] False discovery rate adjusted p-value.

* Number of genes included in the biological process.

patients with malignant ovarian tumors. Our results suggest that the increased Cu content induced VEGF production in the ascitic fluid, which contributed to the progression of ovarian cancer.

Our study showed that elevated Cu levels in ascites are independently associated with malignant ovarian tumor development. Previous studies showed that serum Cu is associated with the development of malignancies, including ovarian tumors [9]. However, ascitic fluid Cu levels in patients with benign and malignant ovarian tumors have not been compared, and the biological relevance of increased ascitic fluid Cu levels has not been reported. Our study revealed that ascitic fluid Cu levels were independently elevated in patients with malignant ovarian tumors. Previous studies have shown that the serum Cu/Zn ratio correlates with the stage of ovarian cancer [22], but the serum Cu levels alone did not correlate with ovarian tumor stage [9]. However, the results from our study suggest that there is a correlation between the serum Cu level in ascites and ovarian cancer stage. Thus, increased Cu levels in ascites may be associated with the prognosis of ovarian cancer.

Our study provides novel evidence that trace elements in ascites and their functions are linked to ovarian cancer and that mesothelial cells are affected by ascites contents. Cu activated pathways and biological processes associated with angiogenesis in ovarian cancer and mesothelial cells; commonly activated pathways include the p53 pathway (P00059) and oxidative stress response (P00046). This is plausible, as Cu induces oxidative stress [23], while these pathways mitigate cellular stress [6]. Furthermore, Cu has been reported to influence biological processes associated with cadmium ion binding in HepG2 cells [24], which is consistent with our findings. The response to cadmium ion (GO:0046686), cellular zinc ion homeostasis (GO:0006882), and cellular transition metal ion homeostasis (GO:0046916) included metallothionein (MT) genes (Supplementary Table S8−10). Genes encoding the metal-binding protein MT were the most responsive to Cu exposure [24–26]. In addition, the pathways and biological processes associated with angiogenesis, which include VEGF, were commonly induced in ovarian cancer and mesothelial cells (Supplementary Tables S8-S10). Angiogenesis is essential for the growth, progression, and metastasis of malignant tumors [27]. This suggests that Cu may be involved in the development of ovarian cancer.

Our findings indicate that the ascitic fluid Cu content might be associated with VEGF production in ascites. To the best of our knowledge, this is the first study to demonstrate a correlation between ascitic fluid VEGF and Cu levels in patients with malignant ovarian tumors. VEGF is the most important factor involved in the promotion of angiogenesis and plays a vital role in the progression of malignant tumors and production of ascites [27]. Ovarian cancer increases the levels of ascitic fluid, which is associated with increased VEGF in and poor prognosis of patients with ovarian cancer [28]. *in vitro* and *in vivo* studies have shown that Cu is associated with VEGF production in cancer [29,30]. Our study showed that the endometrioid A2780 cells were less sensitive to Cu-induced VEGF expression than the serous carcinoma OVCAR3 cells.

Table 6

Thirty most-enriched GO-Slim Biological Processes in Met-5A.

No.	PANTHER GO-Slim Biological Process	Genes *	over +/under -	fold Enrichment	p value[†]
1	response to cadmium ion (GO:0046686)	9	+	25.83	3.52E-07
2	skin development (GO:0043588)	3	+	15.99	2.45E-02
3	protein demethylation (GO:0006482)	5	+	15.55	1.28E-03
4	positive regulation of apoptotic signaling pathway (GO:2001235)	4	+	14.92	6.22E-03
5	epidermal cell differentiation (GO:0009913)	3	+	13.99	3.09E-02
6	cellular zinc ion homeostasis (GO:0006882)	10	+	13.32	3.29E-06
7	response to toxic substance (GO:0009636)	9	+	12.91	1.20E-05
8	positive regulation of angiogenesis (GO:0045766)	3	+	11.19	4.70E-02
9	epidermis development (GO:0008544)	3	+	11.19	4.68E-02
10	extrinsic apoptotic signaling pathway via death domain receptors (GO:0008625)	4	+	9.95	1.79E-02
11	cellular transition metal ion homeostasis (GO:0046916)	10	+	9.33	2.76E-05
12	transition metal ion homeostasis (GO:0055076)	12	+	9.14	3.40E-06
13	'de novo' protein folding (GO:0006458)	5	+	8.88	7.80E-03
14	circadian regulation of gene expression (GO:0032922)	4	+	8.78	2.54E-02
15	negative regulation of MAP kinase activity (GO:0043407)	4	+	8.29	2.88E-02
16	circadian rhythm (GO:0007623)	5	+	7.77	1.27E-02
17	chaperone-mediated protein folding (GO:0061077)	5	+	7.46	1.45E-02
18	positive regulation of programmed cell death (GO:0043068)	12	+	7.34	2.09E-05
19	rhythmic process (GO:0048511)	5	+	7.17	1.65E-02
20	response to metal ion (GO:0010038)	9	+	7.14	4.36E-04
21	negative regulation of MAPK cascade (GO:0043409)	4	+	7.11	4.36E-02
22	positive regulation of cell death (GO:0010942)	12	+	7.11	2.70E-05
23	response to inorganic substance (GO:0010035)	11	+	6.96	8.30E-05
24	epithelial cell differentiation (GO:0030855)	5	+	6.91	1.82E-02
25	positive regulation of apoptotic process (GO:0043065)	11	+	6.84	9.40E-05
26	regulation of apoptotic signaling pathway (GO:2001233)	6	+	6.78	7.69E-03
27	response to hypoxia (GO:0001666)	4	+	6.78	4.84E-02
28	response to oxygen levels (GO:0070482)	4	+	6.78	4.82E-02
29		4	+	6.78	

Table 6 (*continued*)

No.	PANTHER GO-Slim Biological Process	Genes *	over +/under -	fold Enrichment	p value[†]
	response to decreased oxygen levels (GO:0036293)				4.79E-02
30	response to oxidative stress (GO:0006979)	5	+	6.22	2.60E-02

GO, gene ontology.

[†] False discovery rate adjusted p-value.

* Number of genes included in the biological process.

Serous carcinomas often present with peritoneal carcinomatosis, ascites, and advanced stage [31], and VEGF contributes significantly to serous carcinoma progression [32]. In our study, CTR1 was induced in OVCAR3 cells treated with copper but not in A2780 cells (Supplementary table S11−12). A previous study showed that decreased CTR1 expression prevented vascular endothelial cells from taking up copper, resulting in decreased VEGF production [33]. These factors may account for the differences in VEGF expression between the A2780 and OVCAR3 cell lines.

Our study showed that Cu-induced VEGF production in mesothelial cells. Peritoneal mesothelial cells are essential for homeostasis in the abdominal cavity [34]. However, the peritoneum may be significantly involved in the production of ascites, such as through increased permeability in response to VEGF induced by Cu [2]. Cu may be responsible for providing a conducive environment for cancer development in the abdominal cavity. Thus, a Cu chelator may reduce VEGF production in ascites and suppress ovarian cancer progression.

We hypothesized both toxic metals and abnormal levels of the essential metals in ascites were associated with cancer. Although we only investigated the role of Cu based on a preliminary experiment result, changes in the levels of Co, Ni, Zn, As, Se, and Mo may also have

important biological roles for ovarian cancer development. Previous studies have shown that Ni levels were elevated in head and neck cancer and gastrointestinal cancer tissues [36,37]. Ni has been associated with malignant tumor development, through its ability to promote immortalization of epithelial cells and fibroblasts [38,39], as well as DNA methylation [40]. As exposure has been associated with lung and bladder cancer [7], and a previous study showed that As levels were elevated in head and neck cancer tissue [36]. As stimulates the MAP kinase cascade and increases cell proliferation associated with cancer progression [41]. Previous studies have shown that Co levels were elevated in esophageal and colon cancer tissues [37], and it promotes VEGF expression in endothelial cells, supporting tumor expansion [42]. Both low serum Zn levels and low Zn intake are associated with malignant tumors. However, Zn levels were elevated in breast, esophageal, gastric, and colon cancer tissues. [37,43]. Zn accumulation in tumor tissue correlates with increased levels of Zn transporters in tumors, which is a feature of malignancy [43]. Furthermore, Zn promotes vascular endothelial cell proliferation and increases VEGF expression in endothelial and teratocarcinoma cells [44,45]. Oxidative stress occurs as tumor formation progresses. However, driver mutations involved in tumor initiation and progression have been shown to increase antioxidant production to suppress oxidative stress [46,47]. Se is involved in the activity of glutathione peroxidase 4 (GPx4) [48], while Mo is involved in the production of glutathione (GSH) [49], both of which suppress oxidative stress. Elevation of these elements may create an environment that facilitates cancer progression.

In conclusion, our analyses showed that Cu levels are significantly increased in patients with malignant ovarian tumors. We clarified the link between elevated Cu levels in ascites and malignant ovarian tumor progression using microarray analysis, which revealed that Cu activates biological processes promoting angiogenesis and increases extracellular VEGF production in ovarian cancer and peritoneum cells. Cu is also associated with VEGF levels in ascitic fluid from ovarian cancer patients
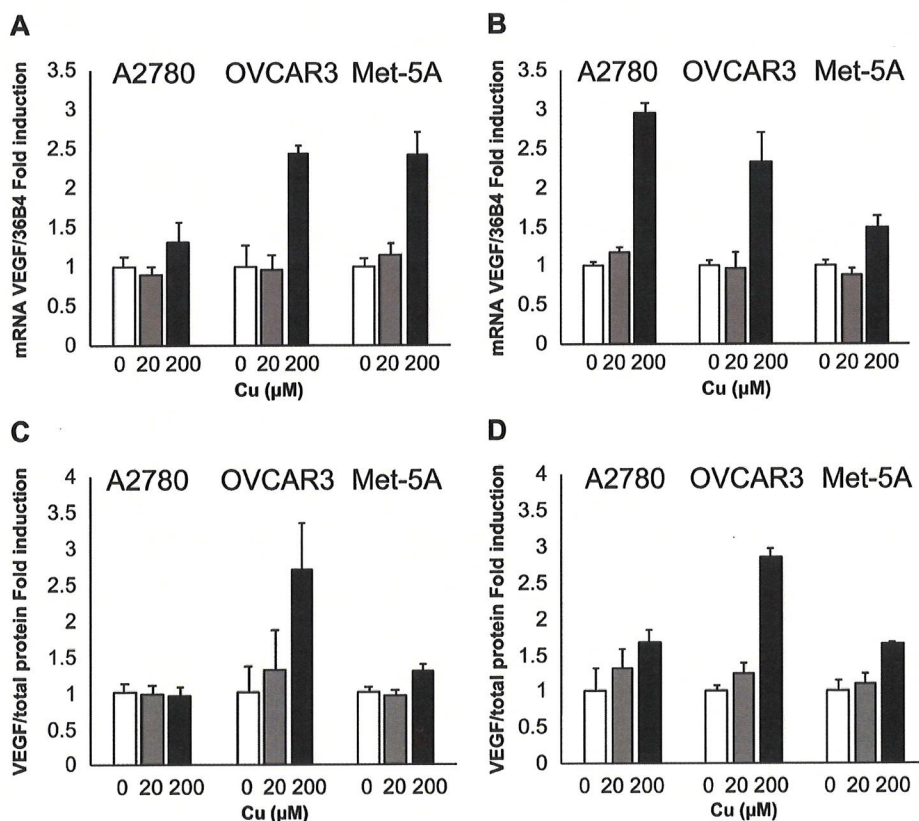

Fig. 2. Cu-induced VEGF extracellular secretion in ovarian cancer and mesothelial cells.

(A) In cells treated with 200 μM Cu for 4 h, VEGF mRNA levels were increased compared to those in cells treated with 0 μM Cu (Dunnett's test; A2780: $p = 0.0216$, OVCAR3: $p < 0.001$. Met-5A: $p = 0.011$). (B) In cells treated with 200 μM Cu for 24 h, VEGF mRNA levels were increased compared to those in cells treated with 0 μM Cu (Dunnett's test; A2780: $p < 0.001$, OVCAR3: $p = 0.003$. Met-5A: $p = 0.002$). (C) In OVCAR3 and Met-5A cells treated with 200 μM Cu for 4 h, the expression of the VEGF protein increased in the supernatant compared with that in the supernatant of cells treated with 0 μM Cu (Dunnett's test; OVCAR3: $p = 0.014$. Met-5A: $p = 0.010$). (D) In cells treated with 200 μM Cu for 24 h, the expression of the VEGF protein was significantly increased in the supernatant compared with that in the supernatant of cells treated with 0 μM Cu (Dunnett's test; A2780: $p = 0.029$, OVCAR3: $p < 0.001$. Met-5A: $p = 0.002$).
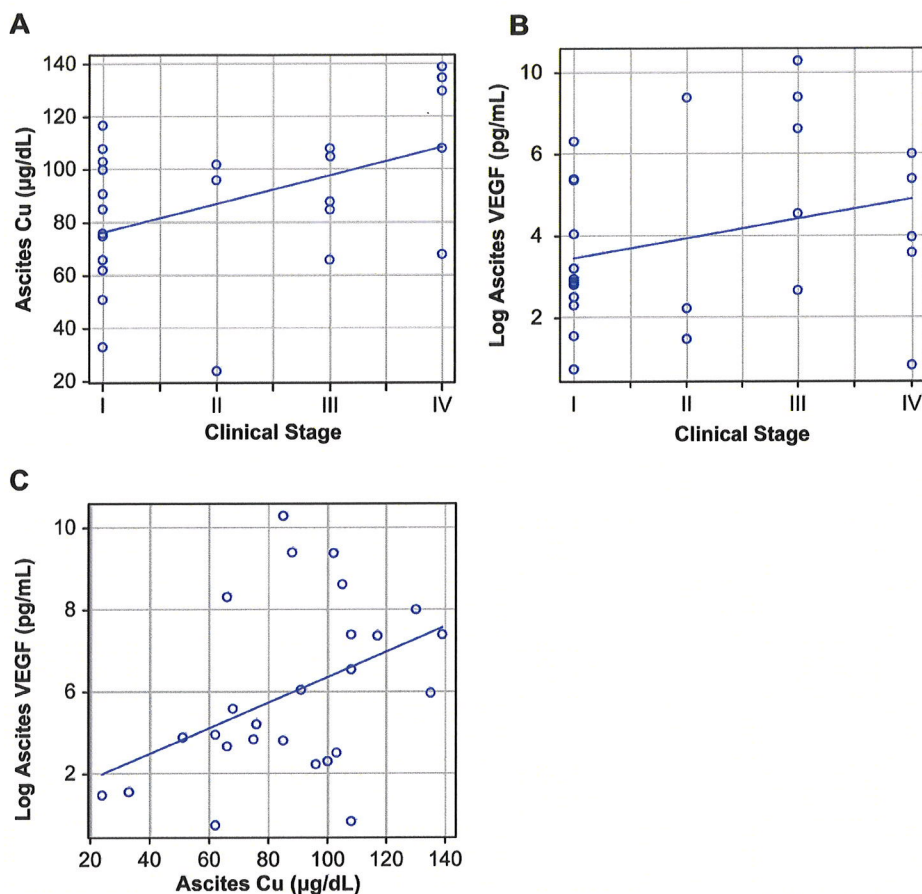
A

B

Fig. 3. Cu concentration in ascitic fluid correlated with the ascitic fluid VEGF level in malignant ovarian tumors.
(A) A significant correlation was observed between ascitic fluid Cu content and clinical stage (Spearman's correlation coefficient 0.445, 95 % CI: 0.069–0.710, $p = 0.023$). (B) Ascitic fluid VEGF values were logarithmically converted. No significant correlation was observed between the clinical stage and ascitic fluid VEGF (Spearman's correlation coefficient 0.279, 95 % CI: -0.122–0.601, $p = 0.168$). (C) Significant correlation was observed between ascitic fluid Cu and VEGF (Spearman's correlation coefficient 0.406, 95 % CI: 0.022–0.686, $p = 0.040$).

C

and may contribute to angiogenesis and ovarian cancer progression. Treatment with Cu chelators may reduce VEGF production and improve the prognosis of ovarian cancer.

Author contributions

Toshimichi Onuma: Conceptualization, Methodology, Software, Formal analysis, Investigation, Resources, Writing - Original Draft, Visualization, Funding acquisition. **Tetsuya Mizutani**: Methodology, Validation, Investigation, Data Curation, Writing - Review & Editing. **Yuko Fujita**: Methodology, Investigation, Resources. **Shizuka Yamada**: Investigation, Resources. **Yoshio Yoshida**: Conceptualization, Supervision, Project administration, Funding acquisition.

Declaration of Competing Interest

The authors declare no potential conflicts of interest.

Appendix A. Supplementary data

Supplementary material related to this article can be found, in the online version, at doi:https://doi.org/10.1016/j.jtemb.2021.126865.

References

[1] A.A. Ayantunde, S.L. Parsons, Pattern and prognostic factors in patients with malignant ascites: a retrospective study, Ann. Oncol. 18 (2007) 945–949.

[2] E. Kipps, D.S.P. Tan, S.B. Kaye, Meeting the challenge of ascites in ovarian cancer: new avenues for therapy and research, Nat. Rev. Cancer 13 (2013) 273–282.

[3] A. Mehri, Trace elements in human nutrition (II) - an update, Int. J. Prev. Med. 11 (2020) 2.

[4] J.-P. Goullé, L. Mahieu, J. Castermant, N. Neveu, L. Bonneau, G. Lainé, D. Bouige, C. Lacroix, Metal and metalloid multi-elementary ICP-MS validation in whole blood, plasma, urine and hair. Reference values, Forensic Sci. Int. 153 (2005) 39–44.

[5] D. Galaris, A. Evangelou, The role of oxidative stress in mechanisms of metal-induced carcinogenesis, Crit. Rev. Oncol. Hematol. 42 (2002) 93–103.

[6] S.S. Leonard, G.K. Harris, X. Shi, Metal-induced oxidative stress and signal transduction, Free Radic. Biol. Med. 37 (2004) 1921–1942.

[7] S.A. Navarro Silvera, T.E. Rohan, Trace elements and cancer risk: a review of the epidemiologic evidence, Cancer Causes Control 18 (2007) 7–27.

[8] H.A. Celik, H.H. Aydin, A. Ozsaran, N. Kilincsoy, Y. Batur, B. Ersoz, Trace elements analysis of ascitic fluid in benign and malignant diseases, Clin. Biochem. 35 (2002) 477–481.

[9] E.J. Margalioth, R. Udassin, C. Cohen, J. Maor, S.O. Anteby, J.G. Schenker, Serum copper level in gynecologic malignancies, Am. J. Obstet. Gynecol. 157 (1987) 93–96.

[10] E. Canaz, M. Kilinc, H. Sayar, G. Kiran, E. Ozyurek, Lead, selenium and nickel concentrations in epithelial ovarian cancer, borderline ovarian tumor and healthy ovarian tissues, J. Trace Elem. Med. Biol. 43 (2017) 217–223.

[11] A. Caglayan, D.C. Katlan, Z.S. Tuncer, K. Yüce, Evaluation of trace elements associated with antioxidant enzymes in blood of primary epithelial ovarian cancer patients, J. Trace Elem. Med. Biol. 52 (2019) 254–262.

[12] B.-E. Kim, T. Nevitt, D.J. Thiele, Mechanisms for copper acquisition, distribution and regulation, Nat. Chem. Biol. 4 (2008) 176–185.

[13] Environmental copper: its dynamics and human exposure issues, J. Toxicol. Environ. Health B Crit. Rev. 4 (2001) 341–394.

[14] A. Gupte, R.J. Mumper, Elevated copper and oxidative stress in cancer cells as a target for cancer treatment, Cancer Treat. Rev. 35 (2009) 32–46.

[15] Y.-Y. Lee, C.H. Choi, I.-G. Do, S.Y. Song, W. Lee, H.S. Park, T.J. Song, M.K. Kim, T.-J. Kim, J.-W. Lee, D.-S. Bae, B.-G. Kim, Prognostic value of the copper transporters,

CTR1 and CTR2, in patients with ovarian carcinoma receiving platinum-based chemotherapy, Gynecol. Oncol. 122 (2011) 361–365.

[16] I. Yajima, N. Uemura, S. Nizam, M. Khalequzzaman, N.D. Thang, M.Y. Kumasaka, A.A. Akhand, H.U. Shekhar, T. Nakajima, M. Kato, Barium inhibits arsenic-mediated apoptotic cell death in human squamous cell carcinoma cells, Arch. Toxicol. 86 (2012) 961–973.

[17] M. Baharvand, S. Manifar, R. Akkafan, H. Mortazavi, S. Sabour, Serum levels of ferritin, copper, and zinc in patients with oral cancer, Biomed. J. 37 (2014) 331–336.

[18] P.D. Thomas, M.J. Campbell, A. Kejariwal, H. Mi, B. Karlak, R. Daverman, K. Diemer, A. Muruganujan, A. Narechania, PANTHER: a library of protein families and subfamilies indexed by function, Genome Res. 13 (2003) 2129–2141.

[19] J. Cai, L. Xia, J. Li, S. Ni, H. Song, X. Wu, Tumor-Associated Macrophages Derived TGF-β–Induced Epithelial to Mesenchymal Transition in Colorectal Cancer Cells through Smad2,3-4/Snail Signaling Pathway, Cancer Res. Treat. 51 (2019) 252–266.

[20] Z. He, A.Y. Chen, Y. Rojanasakul, G.O. Rankin, Y.C. Chen, Gallic acid, a phenolic compound, exerts anti-angiogenic effects via the PTEN/AKT/HIF-1α/VEGF signaling pathway in ovarian cancer cells, Oncol. Rep. 35 (2016) 291–297.

[21] Y. Kanda, Investigation of the freely available easy-to-use software 'EZR'for medical statistics, Bone Marrow Transplant. 48 (2013) 452–458.

[22] A. Lightman, J.M. Brandes, N. Binur, A. Drugan, O. Zinder, Use of the serum copper/zinc ratio in the differential diagnosis of ovarian malignancy, Clin. Chem. 32 (1986) 101–103.

[23] Z. Kang, N. Qiao, G. Liu, H. Chen, Z. Tang, Y. Li, Copper-induced apoptosis and autophagy through oxidative stress-mediated mitochondrial dysfunction in male germ cells, Toxicol. In Vitro 61 (2019), 104639.

[24] C.T. Dameron, M.D. Harrison, Mechanisms for protection against copper toxicity, Am. J. Clin. Nutr. 67 (1998) 1091S–1097S.

[25] M.O. Song, J. Li, J.H. Freedman, Physiological and toxicological transcriptome changes in HepG2 cells exposed to copper, Physiol. Genomics 38 (2009) 386–401.

[26] J. Calvo, H. Jung, G. Meloni, Copper metallothioneins, IUBMB Life 69 (2017) 236–245.

[27] D. Hanahan, R.A. Weinberg, Hallmarks of cancer: the next generation, Cell. 144 (2011) 646–674.

[28] S.K. Chambers, M.C. Clouser, A.F. Baker, D.J. Roe, H. Cui, M.A. Brewer, K. D. Hatch, M.S. Gordon, M.F. Janicek, J.D. Isaacs, A.N. Gordon, R.B. Nagle, H. M. Wright, J.L. Cohen, D.S. Alberts, Overexpression of tumor vascular endothelial growth factor A may portend an increased likelihood of progression in a phase II trial of bevacizumab and erlotinib in resistant ovarian cancer, Clin. Cancer Res. 16 (2010) 5320–5328.

[29] Q. Pan, C.G. Kleer, K.L. van Golen, J. Irani, K.M. Bottema, C. Bias, M. De Carvalho, E.A. Mesri, D.M. Robins, R.D. Dick, G.J. Brewer, S.D. Merajver, Copper deficiency induced by tetrathiomolybdate suppresses tumor growth and Angiogenesis1, Cancer Res. 62 (2002) 4854–4859.

[30] D.C. Rigiracciolo, A. Scarpelli, R. Lappano, A. Pisano, M.F. Santolla, P. De Marco, F. Cirillo, A.R. Cappello, V. Dolce, A. Belfiore, M. Maggiolini, E.M. De Francesco, Copper activates HIF-1α/GPER/VEGF signalling in cancer cells, Oncotarget. 6 (2015) 34158–34177.

[31] U.A. Matulonis, A.K. Sood, L. Fallowfield, B.E. Howitt, J. Sehouli, B.Y. Karlan, Ovarian cancer, Nat. Rev. Dis. Primers 2 (2016) 16061.

[32] B.J. Monk, L.E. Minion, R.L. Coleman, Anti-angiogenic agents in ovarian cancer: past, present, and future, Ann. Oncol. 27 (Suppl 1) (2016) i33–i39.

[33] G. Narayanan, B.S. R, H. Vuyyuru, B. Muthuvel, S. Konerirajapuram Natrajan, CTR1 silencing inhibits angiogenesis by limiting copper entry into endothelial cells, PLoS One 8 (2013), e71982.

[34] S.E. Mutsaers, C.M.-A. Prêle, S. Pengelly, S.E. Herrick, Mesothelial cells and peritoneal homeostasis, Fertil. Steril. 106 (2016) 1018–1024.

[35] S. Hauptmann, K. Friedrich, R. Redline, S. Avril, Ovarian borderline tumors in the 2014 WHO classification: evolving concepts and diagnostic criteria, Virchows Arch. 470 (2017) 125–142.

[36] R. Khlifi, P. Olmedo, F. Gil, B. Hammami, A. Chakroun, A. Rebai, A. Hamza-Chaffai, Arsenic, cadmium, chromium and nickel in cancerous and healthy tissues from patients with head and neck cancer, Sci. Total Environ. 452–453 (2013) 58–67.

[37] F. Nozadi, N. Azadi, B. Mansouri, T. Tavakoli, O. Mehrpour, Association between trace element concentrations in cancerous and non-cancerous tissues with the risk of gastrointestinal cancers in Eastern Iran, Environ. Sci. Pollut. Res. Int. (2021), https://doi.org/10.1007/s11356-021-15224-3.

[38] K.A. Biedermann, J.R. Landolph, Induction of Anchorage Independence in human diploid foreskin fibroblasts by carcinogenic metal Salts1, Cancer Res. 47 (1987) 3815–3823.

[39] S.N. Compounds, Transformation of rat tracheal epithelial cells to immortal growth variants, Mutat. Res. 300 (1993) 179–193.

[40] Y.W. Lee, C.B. Klein, B. Kargacin, K. Salnikow, J. Kitahara, K. Dowjat, A. Zhitkovich, N.T. Christie, M. Costa, Carcinogenic nickel silences gene expression by chromatin condensation and DNA methylation: a new model for epigenetic carcinogens, Mol. Cell. Biol. 15 (1995) 2547–2557.

[41] W. Chen, J.L. Martindale, N.J. Holbrook, Y. Liu, Tumor promoter arsenite activates extracellular signal-regulated kinase through a signaling pathway mediated by epidermal growth factor receptor and Shc, Mol. Cell. Biol. 18 (1998) 5178–5188.

[42] A. Namiki, E. Brogi, M. Kearney, E.A. Kim, T. Wu, T. Couffinhal, L. Varticovski, J. M. Isner, Hypoxia induces vascular endothelial growth factor in cultured human endothelial cells, J. Biol. Chem. 270 (1995) 31189–31195.

[43] S. Alam, S.L. Kelleher, Cellular mechanisms of zinc dysregulation: a perspective on zinc homeostasis as an etiological factor in the development and progression of breast cancer, Nutrients. 4 (2012) 875–903.

[44] D. Zhu, Y. Su, Y. Zheng, B. Fu, L. Tang, Y.-X. Qin, Zinc regulates vascular endothelial cell activity through zinc-sensing receptor ZnR/GPR39, Am. J. Physiol., Cell Physiol. 314 (2018) C404–C414.

[45] S. Hozain, A. Hernandez, J. Fuller, G. Sharp, J. Cottrell, Zinc chloride affects chondrogenesis via VEGF signaling, Exp. Cell Res. 399 (2021), 112436.

[46] Z.T. Schafer, A.R. Grassian, L. Song, Z. Jiang, Z. Gerhart-Hines, H.Y. Irie, S. Gao, P. Puigserver, J.S. Brugge, Antioxidant and oncogene rescue of metabolic defects caused by loss of matrix attachment, Nature. 461 (2009) 109–113.

[47] G.M. DeNicola, F.A. Karreth, T.J. Humpton, A. Gopinathan, C. Wei, K. Frese, D. Mangal, K.H. Yu, C.J. Yeo, E.S. Calhoun, F. Scrimieri, J.M. Winter, R.H. Hruban, C. Iacobuzio-Donahue, S.E. Kern, I.A. Blair, D.A. Tuveson, Oncogene-induced Nrf2 transcription promotes ROS detoxification and tumorigenesis, Nature. 475 (2011) 106–109.

[48] F. Ursini, M. Maiorino, Lipid peroxidation and ferroptosis: the role of GSH and GPx4, Free Radic. Biol. Med. 152 (2020) 175–185.

[49] B.D. Paul, J.I. Sbodio, S.H. Snyder, Cysteine metabolism in neuronal redox homeostasis, trends pharmacol, Sci. 39 (2018) 513–524.

Supplementary Materials

Supplement Table S1. Histological types of ovarian tumor determined using ICP-MS for primary trace element screening in ascites

Histology	n
Benign ovarian tumor	
Endometrial cyst	9
Mature cystic teratoma	7
Serous adenoma	2
Mucinous adenoma	3
Seromucinous adenoma	1
Borderline ovarian tumor	
Borderline malignant mucinous tumor	1
Malignant ovarian tumor	
Clear cell carcinoma	2
Endometrioid carcinoma	2

ICP-MS, inductively coupled plasma mass spectrometry

Supplement Table S2. Histological types of benign ovarian tumor determined using AAS

Histology	% (n)
Endometrial cyst	31.8 (28)
Mature cystic teratoma	30.7 (27)
Serous adenoma	10.2 (9)
Mucinous adenoma	10.2 (9)
Fibroma	6.8 (6)
Paraovarian cyst	4.5 (4)
Sero-mucinous adenoma	2.3 (2)
Adenofibroma	1.1 (1)
Struma ovarii	2.3 (2)

Supplement Table S3. Histological types of borderline ovarian tumor determined using AAS

Histology	%(n)
Mucinous borderline tumor	81.8(9)
Seromuconous borderline tumor	9.1(1)
Sertoli–Leydig cell tumor (moderate differentiated)	9.1(1)

Supplement Table S4. Histological types of malignant ovarian tumor determined using AAS

Histology	% (n)
Serous carcinoma	26.9 (7)
Endometrioid carcinoma	23.1(6)
Clear-cell carcinoma	19.2 (5)
Mucinous carcinoma	11.5 (3)
Seromucinous carcinoma	3.9 (1)
Malignant Brenner tumor	3.9 (1)
Sertoli–Leydig cell tumors (poor differentiated)	3.9 (1)
Neuroendocrine carcinoma	3.9 (1)
Undifferentiated carcinoma	3.9 (1)

Stage	
I	50.0 (13)
II	11.54 (3)
III	19.23 (5)
IV	19.23 (5)

Supplementary Table S5. PANTHER pathway categories identified in A2780

PANTHER pathway	gene	%
Gonadotropin-releasing hormone receptor pathway (P06664)	14	8.4
CCKR signaling map (P06959)	11	6.6
Apoptosis signaling pathway (P00006)	10	6.0
TGF-beta signaling pathway (P00052)	7	4.2
Parkinson disease (P00049)	6	3.6
Ubiquitin proteasome pathway (P00060)	5	3.0
PDGF signaling pathway (P00047)	5	3.0
Huntington disease (P00029)	5	3.0
Angiogenesis (P00005)	4	2.4

p53 pathway (P00059)	4	2.4
Oxidative stress response (P00046)	4	2.4
p38 MAPK pathway (P05918)	4	2.4
EGF receptor signaling pathway (P00018)	4	2.4
Insulin/IGF pathway-mitogen activated protein kinase kinase/MAP kinase cascade (P00032)	3	1.8
Inflammation mediated by chemokine and cytokine signaling pathway (P00031)	3	1.8
FGF signaling pathway (P00021)	3	1.8
VEGF signaling pathway (P00056)	2	1.2
Transcription regulation by bZIP transcription factor (P00055)	2	1.2
Toll receptor signaling pathway (P00054)	2	1.2
Nicotinic acetylcholine receptor signaling pathway (P00044)	2	1.2
Interferon-gamma signaling pathway (P00035)	2	1.2
Thyrotropin-releasing hormone receptor signaling pathway (P04394)	2	1.2
Heterotrimeric G-protein signaling pathway-Gq alpha and Go alpha mediated pathway (P00027)	2	1.2
Heterotrimeric G-protein signaling pathway-Gi alpha and Gs alpha mediated pathway (P00026)	2	1.2
Opioid prodynorphin pathway (P05916)	2	1.2

Pathway		
General transcription regulation (P00023)	2	1.2
Cortocotropin releasing factor receptor signaling pathway (P04380)	2	1.2
Cell cycle (P00013)	2	1.2
Beta3 adrenergic receptor signaling pathway (P04379)	2	1.2
Beta2 adrenergic receptor signaling pathway (P04378)	2	1.2
Beta1 adrenergic receptor signaling pathway (P04377)	2	1.2
5HT4 type receptor mediated signaling pathway (P04376)	2	1.2
Axon guidance mediated by netrin (P00009)	1	0.6
Axon guidance mediated by Slit/Robo (P00008)	1	0.6
Alzheimer disease-presenilin pathway (P00004)	1	0.6
Methionine biosynthesis (P02753)	1	0.6
Heme biosynthesis (P02746)	1	0.6
T cell activation (P00053)	1	0.6
Plasminogen activating cascade (P00050)	1	0.6
PI3 kinase pathway (P00048)	1	0.6
Notch signaling pathway (P00045)	1	0.6
Muscarinic acetylcholine receptor 2 and 4 signaling pathway (P00043)	1	0.6
Metabotropic glutamate receptor group II pathway (P00040)	1	0.6
Synaptic vesicle trafficking (P05734)	1	0.6

GABA-B receptor II signaling (P05731)	1	0.6
Endogenous cannabinoid signaling (P05730)	1	0.6
Metabotropic glutamate receptor group III pathway (P00039)	1	0.6
Androgen/estrogen/progesterone biosynthesis (P02727)	1	0.6
JAK/STAT signaling pathway (P00038)	1	0.6
Ionotropic glutamate receptor pathway (P00037)	1	0.6
Interleukin signaling pathway (P00036)	1	0.6
Integrin signaling pathway (P00034)	1	0.6
p53 pathway by glucose deprivation (P04397)	1	0.6
Hypoxia response via HIF activation (P00030)	1	0.6
Vasopressin synthesis (P04395)	1	0.6
Oxytocin receptor mediated signaling pathway (P04391)	1	0.6
2-arachidonoylglycerol biosynthesis (P05726)	1	0.6
Opioid proopiomelanocortin pathway (P05917)	1	0.6
Opioid proenkephalin pathway (P05915)	1	0.6
Salvage pyrimidine ribonucleotides (P02775)	1	0.6
Enkephalin release (P05913)	1	0.6
Dopamine receptor mediated signaling pathway (P05912)	1	0.6
FAS signaling pathway (P00020)	1	0.6

Angiotensin II-stimulated signaling through G proteins and beta-arrestin (P05911)	1	0.6
Histamine H2 receptor mediated signaling pathway (P04386)	1	0.6
Pyruvate metabolism (P02772)	1	0.6
Pyrimidine Metabolism (P02771)	1	0.6
Endothelin signaling pathway (P00019)	1	0.6
Purine metabolism (P02769)	1	0.6
Cholesterol biosynthesis (P00014)	1	0.6
Blood coagulation (P00011)	1	0.6
B cell activation (P00010)	1	0.6
5HT3 type receptor mediated signaling pathway (P04375)	1	0.6
5HT2 type receptor mediated signaling pathway (P04374)	1	0.6
5HT1 type receptor mediated signaling pathway (P04373)	1	0.6

Supplementary Table S6. PANTHER pathway categories identified in OVCAR3

PANTHER pathway	genes	%
Gonadotropin-releasing hormone receptor pathway (P06664)	28	5.8
CCKR signaling map (P06959)	27	5.6
Apoptosis signaling pathway (P00006)	26	5.4

Integrin signalling pathway (P00034)	25	5.2
EGF receptor signaling pathway (P00018)	19	3.9
Angiogenesis (P00005)	16	3.3
p53 pathway (P00059)	15	3.1
Wnt signaling pathway (P00057)	14	2.9
TGF-beta signaling pathway (P00052)	14	2.9
PDGF signaling pathway (P00047)	13	2.7
Inflammation mediated by chemokine and cytokine signaling pathway (P00031)	13	2.7
Oxidative stress response (P00046)	12	2.5
FGF signaling pathway (P00021)	12	2.5
Parkinson disease (P00049)	11	2.3
Ubiquitin proteasome pathway (P00060)	10	2.1
VEGF signaling pathway (P00056)	10	2.1
Interleukin signaling pathway (P00036)	9	1.9
Ras Pathway (P04393)	9	1.9
p38 MAPK pathway (P05918)	8	1.7
Cadherin signaling pathway (P00012)	7	1.5
Toll receptor signaling pathway (P00054)	6	1.2
Nicotinic acetylcholine receptor signaling pathway (P00044)	6	1.2

Heterotrimeric G-protein signaling pathway-Gq alpha and Go alpha mediated pathway (P00027)	6	1.2
Heterotrimeric G-protein signaling pathway-Gi alpha and Gs alpha mediated pathway (P00026)	6	1.2
Endothelin signaling pathway (P00019)	6	1.2
B cell activation (P00010)	6	1.2
Alzheimer disease-presenilin pathway (P00004)	5	1.0
Alzheimer disease-amyloid secretase pathway (P00003)	5	1.0
Insulin/IGF pathway-mitogen activated protein kinase kinase/MAP kinase cascade (P00032)	5	1.0
p53 pathway feedback loops 2 (P04398)	5	1.0
Huntington disease (P00029)	5	1.0
Blood coagulation (P00011)	5	1.0
Axon guidance mediated by netrin (P00009)	4	0.8
Muscarinic acetylcholine receptor 1 and 3 signaling pathway (P00042)	4	0.8
Thyrotropin-releasing hormone receptor signaling pathway (P04394)	4	0.8
Oxytocin receptor mediated signaling pathway (P04391)	4	0.8
Histamine H1 receptor mediated signaling pathway (P04385)	4	0.8
5HT2 type receptor mediated signaling pathway (P04374)	4	0.8

Axon guidance mediated by Slit/Robo (P00008)	3	0.6
Alpha adrenergic receptor signaling pathway (P00002)	3	0.6
Transcription regulation by bZIP transcription factor (P00055)	3	0.6
T cell activation (P00053)	3	0.6
PI3 kinase pathway (P00048)	3	0.6
Notch signaling pathway (P00045)	3	0.6
Insulin/IGF pathway-protein kinase B signaling cascade (P00033)	3	0.6
FAS signaling pathway (P00020)	3	0.6
Cell cycle (P00013)	3	0.6
Heme biosynthesis (P02746)	2	0.4
Muscarinic acetylcholine receptor 2 and 4 signaling pathway (P00043)	2	0.4
Asparagine and aspartate biosynthesis (P02730)	2	0.4
p53 pathway by glucose deprivation (P04397)	2	0.4
Hypoxia response via HIF activation (P00030)	2	0.4
General transcription by RNA polymerase I (P00022)	2	0.4
Nicotine pharmacodynamics pathway (P06587)	2	0.4
Enkephalin release (P05913)	2	0.4
Dopamine receptor mediated signaling pathway (P05912)	2	0.4
Angiotensin II-stimulated signaling through G proteins and beta-arrestin (P05911)	2	0.4

Cortocotropin releasing factor receptor signaling pathway (P04380)	2	0.4
Cytoskeletal regulation by Rho GTPase (P00016)	2	0.4
Circadian clock system (P00015)	2	0.4
Beta3 adrenergic receptor signaling pathway (P04379)	2	0.4
Beta2 adrenergic receptor signaling pathway (P04378)	2	0.4
Beta1 adrenergic receptor signaling pathway (P04377)	2	0.4
5HT4 type receptor mediated signaling pathway (P04376)	2	0.4
Pentose phosphate pathway (P02762)	2	0.4
5-Hydroxytryptamine degredation (P04372)	2	0.4
Axon guidance mediated by semaphorins (P00007)	1	0.2
Ornithine degradation (P02758)	1	0.2
O-antigen biosynthesis (P02757)	1	0.2
N-acetylglucosamine metabolism (P02756)	1	0.2
Methionine biosynthesis (P02753)	1	0.2
Mannose metabolism (P02752)	1	0.2
Fructose galactose metabolism (P02744)	1	0.2
Formyltetrahydroformate biosynthesis (P02743)	1	0.2
Plasminogen activating cascade (P00050)	1	0.2
De novo purine biosynthesis (P02738)	1	0.2

Coenzyme A biosynthesis (P02736)	1	0.2
Metabotropic glutamate receptor group II pathway (P00040)	1	0.2
Ionotropic glutamate receptor pathway (P00037)	1	0.2
Interferon-gamma signaling pathway (P00035)	1	0.2
Adenine and hypoxanthine salvage pathway (P02723)	1	0.2
Acetate utilization (P02722)	1	0.2
Vitamin D metabolism and pathway (P04396)	1	0.2
Opioid proopiomelanocortin pathway (P05917)	1	0.2
Opioid prodynorphin pathway (P05916)	1	0.2
Glycolysis (P00024)	1	0.2
Opioid proenkephalin pathway (P05915)	1	0.2
General transcription regulation (P00023)	1	0.2
Salvage pyrimidine ribonucleotides (P02775)	1	0.2
Histamine H2 receptor mediated signaling pathway (P04386)	1	0.2
Pyruvate metabolism (P02772)	1	0.2
DNA replication (P00017)	1	0.2
Purine metabolism (P02769)	1	0.2
5HT3 type receptor mediated signaling pathway (P04375)	1	0.2
5HT1 type receptor mediated signaling pathway (P04373)	1	0.2

Supplementary Table S7. PANTHER pathway categories identified in Met-5A

PANTHER pathway	genes	%
Gonadotropin-releasing hormone receptor pathway (P06664)	21	7.4
Apoptosis signaling pathway (P00006)	16	5.7
CCKR signaling map (P06959)	15	5.3
Angiogenesis (P00005)	11	3.9
EGF receptor signaling pathway (P00018)	11	3.9
Integrin signalling pathway (P00034)	10	3.5
p53 pathway (P00059)	9	3.2
Inflammation mediated by chemokine and cytokine signaling pathway (P00031)	8	2.8
FGF signaling pathway (P00021)	8	2.8
TGF-beta signaling pathway (P00052)	8	2.8
PDGF signaling pathway (P00047)	8	2.8
Oxidative stress response (P00046)	8	2.8
VEGF signaling pathway (P00056)	7	2.5
Ras Pathway (P04393)	7	2.5
Interleukin signaling pathway (P00036)	6	2.1
T cell activation (P00053)	6	2.1

Parkinson disease (P00049)	6	2.1
Toll receptor signaling pathway (P00054)	5	1.8
p38 MAPK pathway (P05918)	5	1.8
Nicotinic acetylcholine receptor signaling pathway (P00044)	5	1.8
B cell activation (P00010)	5	1.8
p53 pathway feedback loops 2 (P04398)	4	1.4
Wnt signaling pathway (P00057)	4	1.4
Axon guidance mediated by netrin (P00009)	3	1.1
Insulin/IGF pathway-mitogen activated protein kinase kinase/MAP kinase cascade (P00032)	3	1.1
Hypoxia response via HIF activation (P00030)	3	1.1
Pentose phosphate pathway (P02762)	3	1.1
Huntington disease (P00029)	3	1.1
Heterotrimeric G-protein signaling pathway-Gq alpha and Go alpha mediated pathway (P00027)	3	1.1
Glycolysis (P00024)	3	1.1
PI3 kinase pathway (P00048)	3	1.1
Circadian clock system (P00015)	3	1.1
Fructose galactose metabolism (P02744)	3	1.1

Pathway		
Blood coagulation (P00011)	3	1.1
Beta3 adrenergic receptor signaling pathway (P04379)	2	0.7
Beta2 adrenergic receptor signaling pathway (P04378)	2	0.7
Beta1 adrenergic receptor signaling pathway (P04377)	2	0.7
5HT4 type receptor mediated signaling pathway (P04376)	2	0.7
5HT3 type receptor mediated signaling pathway (P04375)	2	0.7
Alzheimer disease-presenilin pathway (P00004)	2	0.7
5HT2 type receptor mediated signaling pathway (P04374)	2	0.7
5HT1 type receptor mediated signaling pathway (P04373)	2	0.7
Ubiquitin proteasome pathway (P00060)	2	0.7
Heterotrimeric G-protein signaling pathway-Gi alpha and Gs alpha mediated pathway (P00026)	2	0.7
Thyrotropin-releasing hormone receptor signaling pathway (P04394)	2	0.7
Oxytocin receptor mediated signaling pathway (P04391)	2	0.7
FAS signaling pathway (P00020)	2	0.7
Plasminogen activating cascade (P00050)	2	0.7
Endothelin signaling pathway (P00019)	2	0.7
Opioid proopiomelanocortin pathway (P05917)	2	0.7
Opioid prodynorphin pathway (P05916)	2	0.7

Opioid proenkephalin pathway (P05915)	2	0.7
Muscarinic acetylcholine receptor 2 and 4 signaling pathway (P00043)	2	0.7
Dopamine receptor mediated signaling pathway (P05912)	2	0.7
Cortocotropin releasing factor receptor signaling pathway (P04380)	2	0.7
Axon guidance mediated by Slit/Robo (P00008)	1	0.4
Metabotropic glutamate receptor group III pathway (P00039)	1	0.4
Alzheimer disease-amyloid secretase pathway (P00003)	1	0.4
Insulin/IGF pathway-protein kinase B signaling cascade (P00033)	1	0.4
5-Hydroxytryptamine degredation (P04372)	1	0.4
Synaptic vesicle trafficking (P05734)	1	0.4
p53 pathway by glucose deprivation (P04397)	1	0.4
Transcription regulation by bZIP transcription factor (P00055)	1	0.4
Cytoskeletal regulation by Rho GTPase (P00016)	1	0.4
Notch signaling pathway (P00045)	1	0.4
Cell cycle (P00013)	1	0.4
Cadherin signaling pathway (P00012)	1	0.4
Muscarinic acetylcholine receptor 1 and 3 signaling pathway (P00042)	1	0.4
Angiotensin II-stimulated signaling through G proteins and beta-arrestin (P05911)	1	0.4
Metabotropic glutamate receptor group II pathway (P00040)	1	0.4

Supplementary Table S8. DEGs for PANTHER GO-Slim Biological Process in A2780

No	PANTHER GO-Slim Biological Process	DEGs
1	response to cadmium ion (GO:0046686)	*MT1H, MT3, MT1B, MT2A, MT1L, MT1F, MT1M, MT1A, MT1E, MT1M, MT1G*
2	cellular zinc ion homeostasis (GO:0006882)	*SLC30A1, MT1H, MT3, MT1B, MT2A, MT1L, MT1F, MT1M, MT1A, MT1E, MT1M, MT1G*
3	response to toxic substance (GO:0009636)	*MT1H, MT3, MT1B, MT2A, MT1L, MT1F, MT1M, MT1A, MT1E, MT1M, MT1G*
4	chaperone-mediated protein folding (GO:0061077)	*HSPA1A, HSPA6, DNAJB1, HSPA1B, HSPA13, DNAJB4, HSPA2, SMAP1, SGTB*
5	protein demethylation (GO:0006482)	*PHF8, KDM3A, KDM2A, KDM7A*
6	'de novo' protein folding (GO:0006458)	*HSPA1A, HSPA6, DNAJB1, HSPA1B, HSPA13, DNAJB4, HSPA2*
7	cellular transition metal ion homeostasis (GO:0046916)	*FTL, SLC30A1, MT1H, MT3, MT1B, MT2A, MT1L, MT1F, MT1M, MT1A, MT1E, MT1M, MT1G, ABCB6*
8	transition metal ion homeostasis (GO:0055076)	*FTL, SLC30A1, MT1H, MT3, MT1B, MT2A, MT1L, MT1F, MT1M, MT1A, MT1E, HMOX1, MT1M, MT1G, ABCB6*

9	circadian regulation of gene expression (GO:0032922)	CIART, BHLHE40, ID1, ID2
10	negative regulation of MAP kinase activity (GO:0043407)	SPRY4, SPRED3, DUSP1, DUSP5
11	response to metal ion (GO:0010038)	MT1H, MT3, MT1B, MT2A, MT1L, MT1F, MT1M, MT1A, MT1E, MT1M, MT1G
12	response to unfolded protein (GO:0006986)	XBP1, HSPA1A, YOD1, HERPUD1, HSPA6, HSPA1B, HSPA13, HSPA2
13	cellular response to unfolded protein (GO:0034620)	XBP1, HSPA1A, YOD1, HERPUD1, HSPA6, HSPA1B, HSPA13, HSPA2
14	circadian rhythm (GO:0007623)	CIART, BHLHE40, ID1, NFIL3, ID2
15	rhythmic process (GO:0048511)	CIART, BHLHE40, ID1, NFIL3, ID2
16	regulation of angiogenesis (GO:0045765)	VEGFA, PGF, THBS1, GATA2
17	negative regulation of MAPK cascade (GO:0043409)	SPRY4, SPRED3, DUSP1, DUSP5
18	regulation of vasculature development (GO:1901342)	VEGFA, PGF, THBS1, GATA2

19	response to inorganic substance (GO:0010035)	MT1H, MT3, MT1B, OSER1, MT2A, MT1L, MT1F, MT1M, MT1A, MT1E, MT1M, MT1G
20	cellular response to topologically incorrect protein (GO:0035967)	UFD1L, XBP1, HSPA1A, YOD1, HERPUD1, HSPA6, HSPA1B, HSPA13, HSPA2
21	response to topologically incorrect protein (GO:0035966)	UFD1L, XBP1, HSPA1A, YOD1, HERPUD1, HSPA6, HSPA1B, HSPA13, HSPA2
22	regulation of MAP kinase activity (GO:0043405)	SPRY4, SPRED3, GADD45B, SPAG9, TRIB3, DUSP1, DUSP5, GADD45A, TRIB1
23	phospholipid dephosphorylation (GO:0046839)	SYNJ2, MTMR11, SYNJ1, INPP5K, SPP1
24	negative regulation of protein kinase activity (GO:0006469)	SPRY4, SPRED3, CLP1, SH3BP5L, DUSP1, DUSP5
25	negative regulation of protein phosphorylation (GO:0001933)	SPRY4, SPRED3, CLP1, SH3BP5L, INPP5K, DUSP1, DUSP5
26	negative regulation of kinase activity (GO:0033673)	SPRY4, SPRED3, CLP1, SH3BP5L, DUSP1, DUSP5
27	negative regulation of transferase activity (GO:0051348)	SPRY4, SPRED3, CLP1, SH3BP5L, DUSP1, DUSP5

28	negative regulation of phosphorylation (GO:0042326)	*SPRY4, SPRED3, CLP1, SH3BP5L, INPP5K, DUSP1, DUSP5*
29	regulation of protein serine/threonine kinase activity (GO:0071900)	*SPRY4, SPRED3, CLP1, GADD45B, SPAG9, TRIB3, DUSP1, DUSP5, CCNG2, GADD45A, TRIB1*
30	cellular response to external stimulus (GO:0071496)	*NUAK2, SESN2, GABARAPL1, RRAGC, PIEZO2, MAP1LC3B*

DEGs, Differentially Expressed Genes

Supplementary Table S9. DEGs for PANTHER GO-Slim Biological Process in OVCAR3

No	PANTHER GO-Slim Biological Process	DEGs
1	response to cadmium ion (GO:0046686)	*MT1H, MT1B, MT2A, MT1L, MT1F, MT1M, MT1A, MT1E, MT1M, MT1G*
2	regulation of epithelial cell differentiation (GO:0030856)	*MAFF, MAFG, ERRFI1*
3	negative regulation of MAP kinase activity (GO:0043407)	*SPRY4, SPRED3, DUSP6, PTPRJ, SPRED2, DUSP1, DUSP4, DUSP5, SPRED1*
4	epidermis development (GO:0008544)	*OVOL1, MAFF, MAFG, ERRFI1, SCEL*

5	epidermal cell differentiation (GO:0009913)	OVOL1, MAFF, MAFG, ERRFI1
6	peptidyl-tyrosine dephosphorylation (GO:0035335)	UBASH3B, DUSP6, PTPN12, DUSP1, DUSP4, DUSP5
7	negative regulation of MAPK cascade (GO:0043409)	SPRY4, SPRED3, DUSP6, PTPRJ, SPRED2, DUSP1, DUSP4, DUSP5, SPRED1
8	positive regulation of apoptotic signaling pathway (GO:2001235)	FAS, MLLT11, DDIT3, BCL10
9	cellular zinc ion homeostasis (GO:0006882)	SLC30A1, MT1H, MT1B, MT2A, MT1L, MT1F, MT1M, MT1A, SLC30A2, MT1E, MT1M, MT1G
10	signal transduction by p53 class mediator (GO:0072331)	JMY, SPRED3, SPRED2, SPRED1
11	response to toxic substance (GO:0009636)	MT2A, MT1A, MT1L, MT1M, MT1F, MT1G, MT1H, MT1B, MT1E
12	'de novo' protein folding (GO:0006458)	DNAJB1, DNAJB4, HSPA6, HSPE1, HSPA13, HSPA1B, HSPA1A
13	protein demethylation (GO:0006482)	KDM2A, JMJD1C, HR, KDM7A
14	extrinsic apoptotic signaling pathway via death domain receptors	TNFRSF10B, TNFRSF10A, RFFL, DEDD2, TNFRSF10D

	(GO:0008625)	
15	cellular transition metal ion homeostasis (GO:0046916)	*ABCB6, SLC30A2, MT1L, MT1M, SLC30A1, MT2A MT1A, MT1F, MT1G, MT1H, MT1B, FTL, MT1E*
16	chaperone-mediated protein folding (GO:0061077)	*DNAJB1, SGTB, DNAJB4, HSPA6, HSPE1, HSPA13, HSPA1B, HSPA1A*
17	regulation of MAP kinase activity (GO:0043405)	*MAP2K3, SPAG9, DUSP4, MAP2K4, DUSP5, GADD45B, DUSP1, GADD45A, SPRY4, TGFA, PTPRJ, DUSP6, SPRED3, SPRED2, SPRED1, TRIB3, TRIB1*
18	icosanoid metabolic process (GO:0006690)	*PTGES3, AKR1C1, CYP4F2, CYP4F3, AKR1C3*
19	negative regulation of kinase activity (GO:0033673)	*SPRED3, DUSP4, SPRED2, RUBCN, DUSP5, SPRED1, UBASH3B, DUSP1, SPRY4, PTPRJ, CBL, DUSP6*
20	transition metal ion homeostasis (GO:0055076)	*SLC30A2, MT1L, MT1M, SLC30A1, MT2A, MT1A, MT1F, HMOX1, MT1G, MT1H, MT1B, FTL, MT1E*
21	negative regulation of transferase activity (GO:0051348)	*SPRED3, DUSP4, SPRED2, RUBCN, DUSP5, SPRED1, UBASH3B, DUSP1, SPRY4, PTPRJ, CBL, DUSP6*
22	positive regulation of response to DNA damage stimulus (GO:2001022)	*SPRED3, SPRED2, SPRED1, EID3, FXR2*
23	negative regulation of phosphorylation	*DUSP4, RUBCN, DUSP5, DUSP1, SPRY4, PTPRJ, CBL,*

	(GO:0042326)	DUSP6, SPRED3, SPRED2, SPRED1, UBASH3B, PMEPA1, INPP5K
24	negative regulation of protein kinase activity (GO:0006469)	SPRED3, DUSP4, SPRED2, DUSP5, SPRED1, UBASH3B, DUSP1, SPRY4, PTPRJ, CBL, DUSP6
25	negative regulation of protein phosphorylation (GO:0001933)	DUSP4, DUSP5, DUSP1, SPRY4, PTPRJ, CBL, DUSP6, SPRED3, SPRED2, SPRED1, UBASH3B, PMEPA1, INPP5K
26	regulation of apoptotic signaling pathway (GO:2001233)	MLLT11, SRC, DDIT3, FAS, BCL10, RFFL, MCL1, HERPUD1
27	regulation of angiogenesis (GO:0045765)	SPRED1, GATA2, THBS1, PGF, VEGFA
28	epidermal growth factor receptor signaling pathway (GO:0007173)	ERRFI1, SRC, TGFA, CBL, HBEGF
29	regulation of vasculature development (GO:1901342)	SPRED1, GATA2, THBS1, PGF, VEGFA
30	unsaturated fatty acid metabolic process (GO:0033559)	PTGES3, AKR1C1, CYP4F2, CYP4F3, AKR1C3

DEGs, Differentially Expressed Genes

Supplementary Table S10. DEGs for PANTHER GO-Slim Biological Process in Met5A

No	PANTHER GO-Slim Biological Process	DEGs
1	response to cadmium ion (GO:0046686)	*MT2A, MT1A, MT1L, MT1M, MT1F, MT1G, MT1H, MT1B, MT1E*
2	skin development (GO:0043588)	*DSP, ERRFI1, ANXA1*
3	protein demethylation (GO:0006482)	*KDM3A, KDM2A, JMJD1C, KDM7A, PHF8*
4	positive regulation of apoptotic signaling pathway (GO:2001235)	*MLLT11, DDIT3, BCL10, BID*
5	epidermal cell differentiation (GO:0009913)	*ERRFI1, ANXA1, MAFF*
6	cellular zinc ion homeostasis (GO:0006882)	*MT2A, MT1A, MT1L, MT1M, MT1F, MT1G, SLC30A1, MT1H, MT1B, MT1E*
7	response to toxic substance (GO:0009636)	*MT2A, MT1A, MT1L, MT1M, MT1F, MT1G, MT1H, MT1B, MT1E*
8	positive regulation of angiogenesis (GO:0045766)	*ANXA1, GATA2, VEGFA*
9	epidermis development (GO:0008544)	*ERRFI1, ANXA1, MAFF*
10	extrinsic apoptotic signaling pathway via death domain receptors (GO:0008625)	*TNFRSF10B, CFLAR, DEDD2, TNFRSF10D*

11	cellular transition metal ion homeostasis (GO:0046916)	MT2A, MT1A, MT1L, MT1M, MT1F, MT1G, SLC30A1, MT1H, MT1B, MT1E
12	transition metal ion homeostasis (GO:0055076)	MT2A, MT1A, MT1L, MT1M, MT1F, HMOX1, MT1G, SLC30A1, MT1H, MT1B, HMOX2, MT1E
13	'de novo' protein folding (GO:0006458)	DNAJB1, DNAJB4, HSPA6, HSPA1B, HSPA1A
14	circadian regulation of gene expression (GO:0032922)	PER1, BH, HE40, CRY1, BHLHE41
15	negative regulation of MAP kinase activity (GO:0043407)	DUSP4, DUSP5, DUSP1, SPRY4
16	circadian rhythm (GO:0007623)	PER1, NFIL3, BHLHE40, CRY1, BHLHE41
17	chaperone-mediated protein folding (GO:0061077)	DNAJB1, DNAJB4, HSPA6, HSPA1B, HSPA1A
18	positive regulation of programmed cell death (GO:0043068)	MLLT11, ANXA1, STK17A, BNIP3, DDIT3, DAPK3, TNFRSF10B, CFLAR, BCL10, BID, UACA, TNFRSF10D
19	rhythmic process (GO:0048511)	PER1, NFIL3, BHLHE40, CRY1, BHLHE41
20	response to metal ion (GO:0010038)	MT2A, MT1A, MT1L, MT1M, MT1F, MT1G, MT1H, MT1B, MT1E

21	negative regulation of MAPK cascade (GO:0043409)	DUSP4, DUSP5, DUSP1, SPRY4
22	positive regulation of cell death (GO:0010942)	MLLT11, ANXA1, STK17A, BNIP3, DDIT3, DAPK3, TNFRSF10B, CFLAR, BCL10, BID, UACA, TNFRSF10D
23	response to inorganic substance (GO:0010035)	OSER1, MT2A, ANXA1, MT1A, MT1L, MT1M, MT1F, MT1G, MT1H, MT1B, MT1E
24	epithelial cell differentiation (GO:0030855)	TJP1, ERRFI1, ANXA1, MAFF, TJP2
25	positive regulation of apoptotic process (GO:0043065)	MLLT11, ANXA1, STK17A, DDIT3, DAPK3, TNFRSF10B, CFLAR, BCL10, BID, UACA, TNFRSF10D
26	regulation of apoptotic signaling pathway (GO:2001233)	MLLT11, DDIT3, CFLAR, BCL10, BID, HERPUD1
27	response to hypoxia (GO:0001666)	EGLN1, EGLN3, DDIT4, VEGFA
28	response to oxygen levels (GO:0070482)	EGLN1, EGLN3, DDIT4, VEGFA
29	response to decreased oxygen levels (GO:0036293)	EGLN1, EGLN3, DDIT4, VEGFA
30	response to oxidative stress (GO:0006979)	OSER1, ANXA1, GSR, HMOX1, HMOX2

DEGs. Differentially Expressed Genes

Supplementary Table S11. DEGs for OVCAR3 that were not upregulated in A2780

AARS	ABCC1	ABCC3	ABHD16B	ABHD17B	ABHD3	ABL2
ABTB2	ACSL4	ACSS2	ACTR6	ACTRT3	ADAM17	ADAM9
ADM	ADNP2	AFF4	AGFG1	AGO2	AHCYL1	AHR
AKAP13	AKAP2	AKIRIN2	AKR1B10	AKR1C1	AKR1C3	ALDH1L2
ALDH2	AMMECR1	ANKLE2	ANKRD11	ANO6	ANO6	ARAP2
	L					
ARHGAP21	ARHGEF2	ARHGEF26	ARID3B	ARID4B	ARL13B	ARNTL
ARRDC4	ASAP1	ASAP1	ASAP2	ASNS	ASPH	ATF4
ATG14	ATG16L1	ATG16L1	ATP11B	ATP6V1C1	ATP6V1G1	ATRNL1
ATXN1	ATXN1	AUNIP	AZIN1	B4GALNT3	BACH2	BAG1
BAHD1	BAMBI	BCAR3	BCL10	BDNF	BEND4	BEND6
BIN3	BIN3-IT1	BNIP2	C16orf72	C18orf8	C3orf52	C4orf32
C9orf91	CAB39	CABLES1	CACYBP	CALCA	CALD1	CALML5
CAMSAP2	CARD19	CARKD	CASP4	CBFB	CBL	CCDC126
CCDC59	CCDC64	CCK	CCL20	CCNA1	CCND3	CCNYL1
CD44	CDC42EP1	CDK14	CDK17	CDKN1A	CDRT1	CEBPG
CEP170B	CHD1	CHIC2	CHMP2B	CHMP4C	CHRNA5	CHST11

CHST11	CHST15	CLASP2	CLCF1	CLDN1	CLDN16	CLDN4
CLIC4	CLIP4	CMIP	CNKSR3	CNN1	CNN2	CNST
COA6	COBL	COQ10B	CORO1C	COTL1	CPEB2	CPEB3
CREB5	CREM	CRNDE	CRY1	CRYAB	CSRP2	CTAGE5
CTNNAL1	CXCL8	CYP24A1	CYP4F11	CYP4F2	CYP4F3	CYTH1
DAPP1	DCUN1D4	DCUN1D5	DDHD1	DDR2	DENND3	DGKD
DGKD	DGKD	DGKD	DGKD	DGKD	DKK3	DLX1
DLX2	DNAJA1	DNAJA2	DNAJC2	DNAJC6	DNAJC7	DNAJC9
DNMT3B	DNTTIP2	DOPEY2	DSE	DSEL	DST	DUSP14
DUSP4	DUSP6	EBF2	EIF2S2	EIF3F	EIF3F	EIF3F
EIF3J	EIF4EBP1	EIF5	ELF4	ELK3	ELL	ELL2
ELOVL5	EMP1	ENPP2	EPAS1	EPHA2	EPHB2	EPPK1
EPRS	EPT1	ERN1	ERO1B	ERRFI1	ETF1	ETS1
ETS2	ETV4	ETV5	F2RL1	F2RL2	F3	FAM102A
FAM107B	FAM107B	FAM149A	FAM160A1	FAM189A2	FAM210A	FAM27E3
FAM49B	FAM53B	FAM65A	FAM83G	FAS	FAT1	FAT4
FBLIM1	FBXO25	FBXW7	FERMT2	FGF11	FGF2	FKBP4
FLNA	FLNB	FLNC	FLRT2	FLYWCH1	FOSL2	FOXA1
FOXK1	FOXO1	FXR2	FYN	G6PD	GABPB1	GABRE

GARS	GATAD2A	GBE1	GBP1	GCC1	GFPT1	GJB2
GJB3	GJB6	GJC1	GLIPR1	GLIS2	GLS	GMDS
GNA13	GOSR2	GOT1	GP1BB	GPAT3	GPN1	GPR89A
GPRIN1	GRB10	GRHL1	GRPEL2	GSTM3	GTF2IRD1	GTPBP2
HACD1	HGD	HHEX	HIVEP2	HKDC1	HKR1	HLA-B
HMGA1	HNRNPF	HNRNPH1	HOMER2	HOXC13	HPCAL1	HR
HRK	HSPA12A	HSPA4	HSPA4L	HSPA9	HSPB8	HSPD1
HSPE1	ICOSLG	ICOSLG	ID4	IFNE	IGF2BP2	IL18
IL1RAP	IL4R	IL6R	IL6ST	IL7R	INHBE	INSR
IQCJ	IRAK2	IRF2BP2	ISCA1	ITCH	ITGAV	ITGB3
ITGB6	ITPR3	JADE3	JDP2	JMJD1C	JPH3	JUN
JUND	KCNG3	KCNK1	KCNQ3	KCNT2	KCTD10	KCTD11
KCTD15	KCTD9	KDSR	KIAA0232	KIAA0368	KIAA1217	KIF1B
KIF21A	KIF3C	KLF6	KLHL25	KMT5A	KRT17	KRTAP5-AS1
LAMA1	LAMB3	LAMC2	LAMP3	LAMTOR3	LARP4	LARP4B
LARP6	LBR	LCA5	LGALS8	LHFPL2	LIFR	LIMS1
LINC00266-1	LIPG	LITAF	LOC100421561	LONRF3	LRCH1	LRIF1

LRP12	LRRC8C	LRRFIP1	LRRFIP2	LURAP1L	LY6K	LYN
LYST	MAB21L3	MAFK	MALT1	MAP1B	MAP2	MAP2K3
MAP2K4	MAP4	MAPRE3	MARK1	MBOAT2	MBP	MCL1
MCU	MED13	MEF2A	MEGF9	MEMO1	MERTK	METRNL
METTL4	MEX3C	MIB1	MICALL1	MICB	MIR17HG	MLF1
MLXIP	MOB3C	MPP3	MRAS	MREG	MSANTD3	MSANTD3-TMEFF1
MTHFD2	MUM1	MYADM	MYC	MYO1B	MYO5A	NAA20
NAB2	NAMPT	NCAPH2	NCR3LG1	NEDD4	NEXN	NFAT5
NFE2L2	NFKB1	NFKBID	NFKBIZ	NGEF	NIPAL1	NKX2-8
NOCT	NOP58	NPIPA2	NPIPB11	NPIPB15	NPIPB3	NPIPB4
NPIPB4	NPIPB5	NPIPB6	NPIPB8	NPIPB9	NPTN	NR3C1
NRARP	NRCAM	NRG1	NRIP1	NRIP3	NT5C2	NTN4
NUP153	NXT2	OCLN	OGT	OR4F3	ORC6	OSBPL6
OTUB2	OVOL1	PAK1IP1	PALM2-AKAP2	PANK2	PANX2	PAPD7
PAPL	PCK2	PDCD11	PDLIM5	PEA15	PFKP	PHLDA2
PHLPP2	PIEZO1	PIK3CD	PIP4K2A	PISD	PITPNB	PITRM1
PKP4	PLEKHB2	PLEKHF1	PLEKHH2	PLEKHO2	PLRG1	PLXNA2
PLXND1	PMAIP1	PMEPA1	PNPLA2	POPDC3	PPIF	PPP1R14C

PPP1R15B	PPP1R3B	PPP2CB	PPP2R3C	PRELID3A	PREX1	PRKCA
PRKCD	PRKCH	PRKD2	PRNP	PROSER2	PSMD14	PSME4
PTGES3	PTHLH	PTK2	PTPN12	PTPRJ	PTRF	PXDC1
PXK	PYGB	PYROXD1	RAB31	RAB3GAP1	RAB3IP	RAB43
RAB7B	RAD21	RANGAP1	RAP2B	RAPH1	RASAL2	RASGEF1B
RCOR1	RELB	RELT	RFFL	RGPD1	RGPD2	RGPD5
RGPD6	RGPD8	RGS2	RGS20	RHOD	RHOQ	RIOK3
RND3	RNF10	RNF11	RNF114	RNF126	RNF149	RNF19A
RNFT1	RPS6KA3	RPS6KC1	RPUSD4	RRAS2	RRP12	RSL24D1
RTN4	RUBCN	SAMD4A	SAMD4A	SAMD5	SARAF	SARS
SART3	SAV1	SCEL	SCGB3A1	SCP2	SDC3	SDC4
SEC14L1	SELPLG	SEPW1	SERHL	SERINC5	SERPINB5	SERPINB8
SERPINE2	SERPINH1	SERPINH1	SERTAD3	SFN	SGMS2	SGPP2
SH2D4A	SH3BP2	SH3BP5	SH3GL1	SHB	SIAH2	SIPA1L2
SIRT7	SLC10A5	SLC12A7	SLC1A4	SLC1A5	SLC20A1	SLC20A2
SLC22A15	SLC22A5	SLC25A25	SLC26A11	SLC2A1	SLC30A2	*SLC31A1
SLC3A2	SLC41A2	SLC4A7	SLC6A6	SLC6A9	SLC7A1	SLC7A5
SLC9A2	SLCO2A1	SLCO4A1	SMG1	SMOX	SMURF1	SNORD89
SNX16	SNX25	SNX3	SNX9	SOCS2	SORBS1	SOWAHC

SPATS2	SPG20	SPIRE1	SPRED1	SPRED2	SRC	SRF
SRGAP1	SSFA2	STIP1	STK10	STX11	STX6	SUSD5
SVIL	SWAP70	TAF1A	TAGLN	TALDO1	TAOK3	TAP1
TAX1BP1	TBL1X	TCERG1	TCP1	TCP11L2	TGFA	TGFB1
TGIF1	THOC6	THRAP3	TIAM1	TIMM44	TINAGL1	TIPARP
TLE3	TLE4	TLL1	TM2D2	TMEM133	TMEM154	TMEM189
TMEM2	TMEM2	TMEM92	TMX3	TNFAIP1	TNFRSF10A	TNFRSF10B
TNFRSF10D	TNFRSF1A	TNFRSF9	TNPO1	TOP1	TPD52L2	TRAF2
TRAF3	TRIO	TRMO	TRMT10A	TSC22D2	TSKU	TSPAN18
TSPAN9	TTC39B	TTC9	TTL	TTLL3	TUBE1	UAP1
UBAP1	UBASH3B	UBB	UBE2D1	UBE2H	UBL3	UBXN8
UFM1	ULBP1	USP3	USP53	USP7	UXS1	VAPA
VAPA	VASP	VCL	VGLL3	WASF1	WASL	WDR1
WDR43	WNT11	XDH	YARS	YARS	YBX1	YBX3
YWHAG	ZBTB20	ZBTB21	ZBTB7B	ZCCHC6	ZDHHC11	ZDHHC11B
ZDHHC18	ZFAND1	ZFAND3	ZNF165	ZNF280C	ZNF286B	ZNF326
ZNF460	ZNF469	ZNF516	ZNF518B	ZNF57	ZNF805	ZNF829
ZNRF3	ZPR1	ZSCAN31	ZSWIM4			

* Aliases for Copper Transporter 1 (CTR1)

DEGs. Differentially Expressed Genes

Supplementary Table S12. DEGs for A2780 that were not upregulated in OVCAR3

ACADVL	ACOX3	ADPRM	AGPAT4	AKAP17A	ALPK2	ALS2
ANKMY2	ANOS1	AP1S2	AP4B1	APOL2	ARHGAP31	ARHGEF28
ARL4D	ASB3	ASF1A	BABAM1	BAG2	BANP	BCAS2
BCL6	BCLAF1	BEND7	BHLHE40	BTG3	BTN2A2	BTN2A3P
C11orf54	C12orf49	C1S	C2orf42	CA13	CACNA1B	CALB1
CASP8	CBLL1	CBX4	CCBE1	CCDC150	CCDC174	CCDC33
CCDC84	CCDC84	CCDC84	CCDC84	CCDC84	CCDC84	CCNB1IP1
CCNG2	CCNT1	CCPG1	CDKL3	CDKN2AIP	CECR2	CEP97
CEP97	CHMP1B	CIART	CLCN6	CLP1	CLU	COL2A1
COPA	CSAG3	CXCR4	DBF4B	DCDC1	DCTN4	DCUN1D3
DNAJB2	DNAJC7	DNAJC7	DYRK1B	EGR1	ELMSAN1	EPB41L4A
ETV3	EXOC3L1	EXOC7	EXOC8	FAM173B	FAM53C	FLCN
FLJ33534	FNIP1	FOS	FOSB	FXR1	GAN	GBP3
GNPTG	GRN	GRP	GTF2B	GZF1	HEATR4	HELB
HEXA	HNMT	HSD17B7	HSPA2	ID1	ID2	IER2

IER5L	IFNG	IGHMBP2	IL18BP	IQCF3	IRF1	IRF4
ISL2	ITPRIP	KAT7	KDM3A	KDM4A	KDM6A	KEAP1
KLHL15	KLHL24	KMT2D	KMT2E	KPNA1	KPNA3	LIF
LINC01359	LIPH	LMX1A	LOC100129697	LOC100130370	LPIN1	LRRC37B
MAPT	MARVELD3	MBD4	MBNL2	MEF2D	MICA	MID1
MKRN2	MOAP1	MOSPD2	MPZL3	MSMO1	MT3	MTMR11
MTTP	MVD	MYNN	N4BP2L2	NAPB	NEU1	NGDN
NKRF	NPAT	NR4A3	NT5E	NUAK2	OCLM	OR2B6
OTOF	OTUD3	OTUD5	PALLD	PCYT1A	PDCD1LG2	PDCL
PDRG1	PELI1	PGPEP1L	PHF8	PI4K2A	PIAS2	PIEZO2
PKNOX2	PLEKHF2	PLEKHM3	POGZ	POLR1E	PPP4R4	PRKAB2
PSMC4	PSMD11	RABGGTB	RASAL1	RBM24	RBM7	RC3H1
REC8	RFX3	RGS16	RIMKLA	RIMS1	RNMT	RRAGC
RTCA	S100A10	SAMD8	SCPEP1	SDCBP2	SDHAF2	SH3BGR

SH3BP5L	SIGLEC16	SLC10A7	SLC16A1	SLC46A3	SLC51A	SLU7
SMAD6	SMAP1	SMCR8	SMG5	SNAPC4	SP110	SP140L
SP6	SPATS2L	SPTY2D1	SRGN	SRGN	SSX1	SSX2
ST6GALNAC2	STAM	STAM	STOX2	SYDE2	SYNJ1	SYNJ2
TAF4B	TANGO2	TBC1D20	TBK1	TCEAL8	THEM5	TIAL1
TIGD7	TMEM37	TNFAIP3	TNKS2	TOM1	TRAPPC2	TRMT44
TSC22D3	TSGA10	TTC1	TTC1	TUBA4A	TULP4	U2AF2
UBE3B	UBR1	UBR3	UBR4	UMODL1-AS1	UNC5B	USP30
USP32P2	USP49	USPL1	VASN	VPS11	WBP2	WDR74
WDR91	YEATS4	YOD1	ZBTB34	ZBTB49	ZBTB5	ZC3HAV1
ZFAT	ZFP36L1	ZFP37	ZNF10	ZNF175	ZNF189	ZNF222
ZNF224	ZNF227	ZNF234	ZNF235	ZNF275	ZNF324	ZNF383
ZNF384	ZNF419	ZNF461	ZNF48	ZNF484	ZNF547	ZNF548
ZNF583	ZNF688	ZNF711	ZNF780B	ZNF791	ZSCAN9	

DEGs. Differentially Expressed Genes

Supplementraly Figure S8

OvarianTumor